POLITECNICO DI TORINO
Repository ISTITUZIONALE

Self-influenced growth through evolving material inhomogeneities

Original
Self-influenced growth through evolving material inhomogeneities / DI STEFANO, Salvatore; Ramírez-Torres, Ariel; Penta, Raimondo; Grillo, Alfio. - In: INTERNATIONAL JOURNAL OF NON-LINEAR MECHANICS. - ISSN 0020-7462. - 106:(2018), pp. 174-187. [10.1016/j.ijnonlinmec.2018.08.003]

Availability:
This version is available at: 11583/2720455 since: 2020-06-03T17:18:55Z

Publisher:
Elsevier Ltd

Published
DOI:10.1016/j.ijnonlinmec.2018.08.003

Terms of use:

This article is made available under terms and conditions as specified in the corresponding bibliographic description in the repository

Publisher copyright
Elsevier postprint/Author's Accepted Manuscript

© 2018. This manuscript version is made available under the CC-BY-NC-ND 4.0 license
http://creativecommons.org/licenses/by-nc-nd/4.0/.The final authenticated version is available online at:
http://dx.doi.org/10.1016/j.ijnonlinmec.2018.08.003

(Article begins on next page)

25 April 2024

Self-influenced growth through evolving material inhomogeneities

Salvatore Di Stefano[a], Ariel Ramírez-Torres[a], Raimondo Penta[b], Alfio Grillo[a,*]

[a] *Dipartimento di Scienze Matematiche (DISMA) "G.L. Lagrange", Politecnico di Torino, Corso Duca degli Abruzzi 24, 10129, Torino, Italy*
E-mail: {salvatore.distefano ariel.ramirez alfio.grillo}@polito.it
[b] *School of Mathematics and Statistics, Mathematics and Statistics Building, University of Glasgow, University Place, Glasgow G12 8QQ, UK*
E-mail: Raimondo.Penta@glasgow.ac.uk

Abstract

We reformulate a model of avascular tumour growth in which the tumour tissue is studied as a biphasic medium featuring an interstitial fluid and a solid phase. The description of growth relies on two fundamental features: One of those is given by the mass transfer among the constituents of the phases, which is taken into account through source and sink terms; the other one is the multiplicative decomposition of the deformation gradient tensor of the solid phase, with the introduction of a *growth tensor*, which represents the growth-induced structural changes of the tumour. In general, such tensor is non-integrable, and it may allow to define a Levi-Civita connection with non-trivial curvature. Moreover, its evolution is related to the source and sink of mass of the solid phase through an evolution equation. Our goal is to study how growth can be influenced by the inhomogeneity of the growth tensor. To this end, we study the evolution of the latter, as predicted by two different models. In the first one, the dependence of the growth tensor on the tumour's material points is not explicitly considered in the evolution equation. In the second model, instead, the inhomogeneity of the growth tensor is resolved explicitly by introducing the curvature associated with it into the evolution equation. Through numerical simulations, we compare the results produced by these two models, and we evaluate a possible role of the material inhomogeneities on growth.

Keywords: Growth, Remodelling, Material inhomogeneities, Inelastic distortions
2010 MSC: 74Bxx, 74Cxx, 74Fxx, 76Sxx, 76Zxx, 92Bxx

☆Submitted to the Special Issue "Constitutive Modelling in Biomechanics"

*Corresponding author
Email address: alfio.grillo@polito.it (Alfio Grillo)

1. Introduction

Because of its repercussion on public health, the study of tumour growth is a very active research field, to which mathematical modelling can give an important contribution [1, 2, 3]. A rather standard approach is to answer specific questions at each scale of interest by formulating dedicated models. These can be based on Statistical Mechanics [4], Kinetic Theories[5, 6, 7, 8, 9], and Continuum Mechanics [10, 11] (and references therein), depending on whether the given problem involves the molecular, cellular, or the tissue scale. One of the main challenges, however, is to understand the complexes of phenomena that contribute to initiate the sprouting of a tumour, and to bridge across the physical scales at which they occur. The difficulty arises, for instance, when different types of models, conceived for different scales and disciplines, have to be combined efficiently, and solved simultaneously.

Within the framework of Continuum Mechanics, the search for the multi-scale and interdisciplinary approach outlined above is put into action by formulating multiphasic, multi-scale models of tumour growth (see e.g. [12, 13, 14, 15, 16, 17]). In such models, growth is described as the mass variation of the solid phase of the tumour at the expenses of its fluid constituents, and the mass variation is often viewed as the result of the cooperation of both chemical ad mechanical factors [18].

From the point of view of Mechanics, a relevant aspect of growth is the occurrence of structural transformations that accompany the "*visible*" motion of a tissue [19, 20] as well as its gain or loss of mass. All through the years, a huge amount of literature has been produced on this subject, and on the related issue of the residual stresses and strains that are expected to exist in a grown material [21]. In fact, apart from [22] and some other recent papers (see e.g. [23]), many works usually address the structural evolution of a medium that grows or remodels by having recourse to the Bilby-Kröner-Lee decomposition (BKL-decomposition) of the deformation gradient tensor (see e.g. [10, 15, 19, 24, 25, 26, 27, 28, 29, 30, 31, 32, 33, 34, 35] and the references therein). For a historically reliable review on the roots of the BKL decomposition and on its significance in Differential Geometry, the Reader is referred to [36] (Chapter 1, pp. 10–27) and to [37]. In both cases, the Authors give due credit to the "old", yet always up-to-date, ideas that have led to what we nowadays know as BKL decomposition. In particular, the review provided in [37] makes the uncommon effort of drawing the attention of the Reader on some literature that, in spite of its importance, has not become as popular as it deserved.

In the case of growth, the simplest version of the BKL-decomposition consists of splitting the deformation gradient tensor of a tissue into an ac-

commodating factor and a growth factor (cf. Sect. 2). The latter one, denoted by $\boldsymbol{F}_\gamma$ in the following, is often referred to as *growth tensor*, and is taken as the representative of the changes of the tissue's internal structure.

The main properties of $\boldsymbol{F}_\gamma$ are that it is non-integrable in general, and that it may induce a non-Euclidean metric tensor, $\boldsymbol{C}_\gamma = \boldsymbol{F}_\gamma^{\mathrm{T}}.\boldsymbol{F}_\gamma$. The latter can be employed to construct a Levi-Civita connection with a non vanishing fourth-order curvature tensor, $\boldsymbol{\mathcal{R}}$. This result is consistent with the analysis of Kröner [38], according to whom the stress-free body pieces can be glued together in a non-Euclidean space. We emphasise that, in the context of growth, the concept of curvature has been explored e.g. in [39, 40, 41, 42, 43, 44, 45] (see also [46]).

The introduction of the growth tensor, $\boldsymbol{F}_\gamma$, produces many similarities among growth, finite strain elastoplasticity, and the theory of defects in solids (see e.g. [47, 36] for a review) and, in fact, many biological aspects of growth can be re-interpreted in terms of the evolution of inelastic distortions. One similarity with elastoplasticity is the definition of a stress-free "intermediate configuration", which exemplifies the conceptual separation between growth and deformation. Actually, the "intermediate configuration" is a collection of tissue pieces rather than a true configuration, and is obtained in two steps: First, by removing all the loads acting on the current configuration of the tissue, and then, by ideally chopping the tissue in small, stress-free pieces [36]. These can be assembled in a reference configuration by means of a transformation that is identifiable with $\boldsymbol{F}_\gamma^{-1}$. Hence, growth can be understood as the reverse process, which maps the tissue pieces from the reference configuration into the intermediate one.

Tensor $\boldsymbol{F}_\gamma^{-1}$ is *formally* related to the existence of growth-induced inhomogeneities, [28, 42, 48, 49]. Note that we have emphasised the adverb "formally" because, in our theory, we are not using the concept of "*archetype*" [42, 48, 49]. This notion, instead, is used to define an inhomogeneous body as a body for which it is possible to define a non-singular tensor field, whose inverse is non-integrable [28, 42].

Clearly, the way in which the inhomogeneities evolve depends on the biological problem under study and, thus, on the proposed model of growth. For instance, in [28], a prototypal evolution law for the growth inhomogeneities is set in the form of a relation between Eshelby stress and the rate at which the inhomogeneities themselves are produced. In this case, the evolution law is obtained by following a reduction procedure that requires its compliance with the body's material symmetries, and with the principles of uniformity, objectivity, and independence of the reference configuration [28].

A different perspective is considered e.g. in [29, 50], where some phenomenological growth laws are discussed within a chemo-mechanical frame-

work. For arteries [51], an evolution law for the growth tensor is obtained in terms of a generalised Onsager's relation, in which the driving force of growth is identified with the difference between a suitable measure of mechanical stress and a target stress, referred to as "*homeostatic stress*".

As long as tumour growth is concerned, the hypothesis is often made that the growth tensor is a pure dilatation [52, 53], therby depending on one parameter only, denoted by γ and referred to as "growth parameter" in the sequel. In such cases, one has to supply an evolution law for γ (see e.g. (11b) below), which translates the mass balance law for the tissue's solid phase into a kinematic constraint on γ itself [54, 55, 56, 57]. When this line of thought is followed, the evolution of the growth tensor is entirely dictated by the law describing the variation of mass of the tissue, denoted by r_{s} in our notation.

Since r_{s} is related to the rate of change of γ, the problem arises to determine a generalised force that is conjugate to the variation of γ and that, thus, triggers growth. However, since r_{s} is almost always assigned on the basis of biological observations (see e.g. [55, 56]), which may be phenomenological or "*micro-mechanically motivated*" [10], it may not be possible to identify mechanical stress with the "driving force" that moves the growth-related distortions (i.e., the inhomogeneities, in the jargon of [28, 42]). This is, in fact, a relevant difference with elastoplasticity, in general, and with the models put forward in [28, 51], in which stress plays a central role. Indeed, it should be emphasised that the growth of a tumour may occur also in the absence of stress, whereas it strongly depends on the presence of nutrients, and may result in a loss of mass when these are unavailable. Still, stress may contribute to modulate the way in which the mass change takes place [54, 58]. Perhaps, we might say that, whereas stress is the "starring character" of pure remodelling (be it growth-induced or not), as it can be the trigger of the changes of the tissue's structure, it is somehow "downgraded" to a modulating factor in the case of pure growth[1].

A rather different approach is suggested in [42], where the concept of "*self-driven*" inhomogeneities is introduced. The underlying idea, framed within the theory of defects in solids, could be rephrased as follows. Assume to have an inhomogeneous solid medium with a non-uniform distribution of defects, which can be modelled as incompatible distortions, and thus associated with $\boldsymbol{F}_\gamma$. Assume, in addition, that the defects interact with each other, and that the strength of their mutual interaction is accounted for by the variability of $\boldsymbol{F}_\gamma$ (i.e., the more $\boldsymbol{F}_\gamma$ varies, the stronger the interaction is). Then, to adhere to Epstein's statement [42]:

[1]We warmly thank Prof. Luigi Preziosi for several discussions on this issue.

> "*The evolution is* intrinsic *or* self-driven *if* [...] *the inhomogeneity moves just by virtue of its being there, perhaps in its effort to relax itself*"

we claim that the spatial variability of $\boldsymbol{F}_\gamma$ is sufficient to initiate a spontaneous evolution of $\boldsymbol{F}_\gamma$ in time.

In our work, we formulate a model of tumour growth based on the theory presented in [42, 54]. We are interested in quantifying how, and to what extent, the inhomogeneities produced by growth influence the spatiotemporal evolution of γ. For this purpose, we propose a model that merges the quasi-phenomenological definition of r_s supplied in [54] with the concept of "*self-driven*" distortions put forward in [42]. The underlying idea is that the functional form of the source/sink of mass r_s should be modified by introducing a term that takes explicitly into account the scalar curvature, κ_γ, associated with $\boldsymbol{\mathcal{R}}$ (see Sect. 2.2). Our motivation for undertaking this task, inspired by [42], is to give a possible answer to the following question:

> Let us "prepare" the tissue in some grown configuration, with initial distribution of γ, γ_in, corresponding to nonzero curvature, $\kappa_{\gamma\mathrm{in}}$. Then, giving for granted that growth produces inhomogeneities [28, 42], what is the impact of the initial inhomogeneities on the growth of the tissue in the subsequent instants of time?

The remainder of this work is structured as follows: In Sect. 2, we provide the notation and the fundamental definitions used in our work. In Sect. 3, we formulate in detail our model of tumour growth. In Sect. 4, we solve a benchmark problem. In Sect. 5, we comment the results of our numerical simulations and, finally, in Sect. 6, we summarise our results, and outline some future research goals.

2. Theoretical background

2.1. Kinematics of growth

We indicate by $\mathscr{B}$ a bounded region of the three-dimensional Euclidean space, $\mathscr{S}$, chosen as reference placement for the considered tissue. For every $X \in \mathscr{B}$ and every $x \in \mathscr{S}$, we introduce the tangent spaces $T_X\mathscr{B}$ and $T_x\mathscr{S}$ and the tangent bundles $T\mathscr{B} = \sqcup_{X\in\mathscr{B}} T_X\mathscr{B}$ and $T\mathscr{S} = \sqcup_{x\in\mathscr{S}} T_x\mathscr{S}$. Moreover, we denote by $\mathscr{B}(t) \equiv \chi(\mathscr{B}, t)$ the placement of the tissue at time $t \in \mathscr{I}$, where $\chi(\,\cdot\,, t) : \mathscr{B} \to \mathscr{S}$ is the *motion* and $\mathscr{I} \subset \mathbb{R}$ an interval of time. The tangent map $\boldsymbol{F}(\,\cdot\,, t) \equiv T\chi(\,\cdot\,, t)$ is the deformation gradient tensor, and is defined as $\boldsymbol{F}(\,\cdot\,, t) : T\mathscr{B} \to T\mathscr{S}$, so that, for every $X \in \mathscr{B}$, $\boldsymbol{F}(X, t)$ maps vectors of $T_X\mathscr{B}$ into vectors of $T_{\chi(X,t)}\mathscr{S}$, i.e., $\boldsymbol{F}(X, t) : T_X\mathscr{B} \to T_{\chi(X,t)}\mathscr{S}$.

Remark 1. *The "classical" definition of reference placement, or configuration, although widely used in Solid Mechanics, may not apply to biological tissues. To the best of our knowledge, this is particularly true for a medium undergoing appositional growth, i.e., the process in which material particles are either deposited on the growing medium, or depleted from it. In both cases, the "number" of material particles constituting the medium varies with time and, consequently, it is impossible to define a unique reference configuration for the medium, at least in the classical sense [22]. Rather, as reported in [22],* "the reference configuration of a material point is defined at the time it is deposited," *which means that, at different times, the medium has to be associated with different reference configurations. In our setting, however, we deal with volumetric growth. This type of growth, in fact, still permits the definition of a fixed reference configuration for a growing medium if, as stated in [28], the addition or depletion of material is assumed to occur* "in such a way that material points preserve their identity"*. With the aid of this hypothesis, we can assume the existence of a fixed reference configuration for the medium under investigation.*

A major character of our theory is the BKL-decomposition, $\boldsymbol{F} = \boldsymbol{F}_{\mathrm{e}}\boldsymbol{F}_{\gamma}$. As anticipated in the Introduction, $\boldsymbol{F}_{\gamma}$ describes the inelastic changes of the tissue's internal structure that are induced by growth, while $\boldsymbol{F}_{\mathrm{e}}$ is the accommodating part of $\boldsymbol{F}$, and is assumed to be elastic. Both $\boldsymbol{F}_{\mathrm{e}}$ and $\boldsymbol{F}_{\gamma}$ are non-singular, and their determinants, $J_{\mathrm{e}} = \det \boldsymbol{F}_{\mathrm{e}}$ and $J_{\gamma} = \det \boldsymbol{F}_{\gamma}$, are strictly positive.

For every pair $(X, t) \in \mathscr{B} \times \mathscr{I}$, we prescribe that $\boldsymbol{F}_{\gamma}(X, t)$ maps vectors of $T_X\mathscr{B}$ into "relaxed" vectors of another tangent space. Such space is denoted by $T_X\mathscr{N}_t$, and can be identified with the image of $T_X\mathscr{B}$ through $\boldsymbol{F}_{\gamma}(X, t)$ [45]. Coherently, we write $\boldsymbol{F}_{\gamma}(X, t) : T_X\mathscr{B} \to T_X\mathscr{N}_t$, and, putting together this result and the definition of $\boldsymbol{F}(X, t)$, we express the elastic part of $\boldsymbol{F}(X, t)$ as $\boldsymbol{F}_{\mathrm{e}}(X, t) : T_X\mathscr{N}_t \to T_{\chi(X,t)}\mathscr{S}$.

In general, the tissue may find itself in a stressed state both in the current and in the reference configuration. Stresses may have different origin but, in the present context, they are generated either by growth or by the loading history undergone by the tissue. Since in our framework growth is the only process regarded as inelastic, it produces stresses that cannot be eliminated by simply switching off the applied loads. Indeed, even though all such loads were suppressed, the tissue would still occupy a configuration in which the growth-induced stresses are nonzero.

As mentioned in the Introduction, to achieve a state in which every part of the tissue is free of stress, one should virtually disassemble the tissue into a *"conglomerate"* of completely relaxed pieces [38]. Each of such pieces can

be thought of as an arbitrarily small neighbourhood of a point $x \in \mathscr{B}_t$, and, for infinitesimally small neighbourhoods, the body piece associated with x can be identified with the tangent space of $\mathscr{B}_t$ at x, i.e., $T_x\mathscr{B}_t$. In this case, the whole relaxation can be viewed as a linear mapping between tangent spaces. In particular, since the relaxation is elastic, it is represented by $\boldsymbol{F}_{\mathrm{e}}^{-1}(x,t) : T_x\mathscr{B}_t \to T_X\mathscr{N}_t$.

Although, $T_X\mathscr{N}_t$ is attached to the same point $X \in \mathscr{B}$ as $T_X\mathscr{B}$, it depends on time and, above all, it is associated with a state of the tissue characterised by an important property: it is free of stress, and is obtained by distorting the elements of $T_X\mathscr{B}$, or the elements of $T_x\mathscr{B}_t$, in a generally incompatible way. Hence, neither $\boldsymbol{F}_\gamma(X,t)$ nor $\boldsymbol{F}_{\mathrm{e}}^{-1}(x,t)$ can be taken as the tangent maps of deformations evaluated at $X \in \mathscr{B}$ and $x \in \mathscr{B}_t$, respectively. Since this reasoning applies for each $X \in \mathscr{B}$, the tangent bundle $T\mathscr{N}_t = \sqcup_{X\in\mathscr{B}} T_X\mathscr{N}_t$ cannot be associated with a configuration in the Euclidean space, and $\mathscr{N}_t$ cannot be claimed to be a configuration in the classical sense. Rather, it is the *natural*, or ground, state of the tissue, i.e., the state in which the tissue is free of stress. Such state encompasses the whole structural evolution undergone by the tissue, which occurs from the reference configuration in the form of the distortional tensor map $\boldsymbol{F}_\gamma(\,\cdot\,,t) : T\mathscr{B} \to T\mathscr{N}_t$. A sketch of the explanation given so far is given in Fig. 1 (left), where $\mathscr{N}_t$ is represented as a *"conglomerate"* of stress-free body pieces [38]. We recall, however, that $\mathscr{N}_t$ can be assembled in a stress-free Riemannian manifold, endowed with the curved metric induced by $\boldsymbol{F}_\gamma$ (cf. e.g. [38, 39, 45]).

We notice that, at this stage, $\boldsymbol{F}_\gamma$ is not subjected to any restriction. Hence, granted the polar decompositions $\boldsymbol{F}_\gamma(X,t) = \boldsymbol{R}_\gamma(X,t)\boldsymbol{U}_\gamma(X,t)$ and $\boldsymbol{F}_\gamma(X,t) = \boldsymbol{V}_\gamma(X,t)\boldsymbol{R}_\gamma(X,t)$, which hold true for each pair $(X,t) \in \mathscr{B} \times \mathscr{I}$, $\boldsymbol{F}_\gamma(X,t)$ is generally obtained by combining one of the inelastic stretches, $\boldsymbol{U}_\gamma(X,t) : T_X\mathscr{B} \to T_X\mathscr{B}$ and $\boldsymbol{V}_\gamma(X,t) : T_X\mathscr{N}_t \to T_X\mathscr{N}_t$, with the rotation tensor $\boldsymbol{R}_\gamma(X,t) : T_X\mathscr{B} \to T_X\mathscr{N}_t$.

Before going further, we mention that a different formulation of the BKL-decomposition is presented in [59, 60]. The core of such formulation is the use of two mappings that define a base and a *"target"* [60] configuration for each of the factors of the BKL-decomposition. In summary, one indicates by $\boldsymbol{F}_{\mathrm{a}}$ and $\boldsymbol{F}_{\mathrm{g}}$ the accommodating and the growth part of $\boldsymbol{F}$, so that $\boldsymbol{F} = \boldsymbol{F}_{\mathrm{a}}\boldsymbol{F}_{\mathrm{g}}$ holds true, and introduces the differentiable mappings χ_{a} and χ_{g} such that $\boldsymbol{F}_{\mathrm{a}}$ and $\boldsymbol{F}_{\mathrm{g}}$ are expressed as $\boldsymbol{F}_{\mathrm{a}} = (T\chi_{\mathrm{a}})\boldsymbol{H}_{\mathrm{a}}$ and $\boldsymbol{F}_{\mathrm{g}} = (T\chi_{\mathrm{g}})\boldsymbol{H}_{\mathrm{g}}$ [60]. Here, $T\chi_{\mathrm{a}}$ and $T\chi_{\mathrm{g}}$ are the tangent maps of χ_{a} and χ_{g}, and they represent the *compatible* contributions to $\boldsymbol{F}_{\mathrm{a}}$ and $\boldsymbol{F}_{\mathrm{g}}$. On the contrary, in general $\boldsymbol{H}_{\mathrm{a}}$ and $\boldsymbol{H}_{\mathrm{g}}$ cannot be identified with the tangent map of any deformation. Indeed, $\boldsymbol{H}_{\mathrm{g}}$ describes the generally *incompatible* structural changes due to growth, while $\boldsymbol{H}_{\mathrm{a}}$ models the elastic distortions that may have to be applied to the

grown body pieces to restore a global configuration.

For every $t \in \mathscr{I}$, the map $\chi_{\mathrm{g}}(\,\cdot\,,t)$ is identified with the diffeomorphism $\chi_{\mathrm{g}}(\,\cdot\,,t) : \mathscr{B} \to \mathscr{C}_t$, where $\mathscr{C}_t$ is referred to as *"intermediate configuration"*, while $T\chi_{\mathrm{g}}(\,\cdot\,,t)$ and $\boldsymbol{H}_{\mathrm{g}}(\,\cdot\,,t)$ are defined in terms of maps between tangent spaces, i.e., $T\chi_{\mathrm{g}}(X,t) : T_X\mathscr{B} \to T_{\chi_{\mathrm{g}}(X,t)}\mathscr{C}_t$ and $\boldsymbol{H}_{\mathrm{g}}(X,t) : T_X\mathscr{B} \to T_X\mathscr{B}$, respectively [60]. Analogous considerations hold for $\chi_{\mathrm{a}}(\,\cdot\,,t) : \mathscr{C}_t \to \mathscr{B}_t$ and for $T\chi_{\mathrm{a}}(\,\cdot\,,t)$, and $\boldsymbol{H}_{\mathrm{a}}(\,\cdot\,,t)$ (see [60] for details). A drawing summarising the view of the BKL-decomposition presented in [60] is given in Fig. 1 (right). We notice that $\boldsymbol{H}_{\mathrm{g}}$ plays the same role as $\boldsymbol{F}_\gamma$ in the present context.

We emphasise that, although we do not use here the approach by [60], we find it important to draw attention on it because, through χ_{g} (or χ_{a}), it introduces an additional degree of freedom that, along with $\boldsymbol{F}_\gamma$, could be useful for other applications of the BKL-decomposition.

In the following, we investigate some consequences of the generally non-integrable nature of $\boldsymbol{F}_\gamma$ on the evolution of growth itself (cf. also [39, 45]).

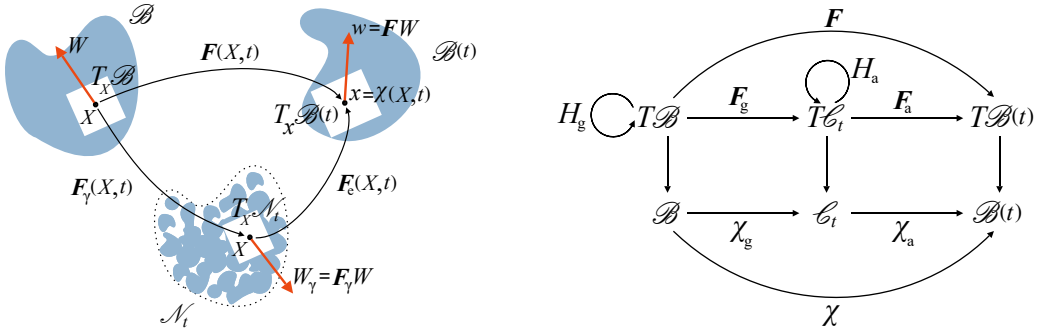

Figure 1: Schematic representation of the introduced mappings.

2.2. Growth and curvature

In this work, $\boldsymbol{F}_\gamma$ is assumed to induce the Riemannian metric tensor

$$\boldsymbol{C}_\gamma = \boldsymbol{F}_\gamma^{\mathrm{T}}.\boldsymbol{F}_\gamma, \tag{1}$$

with is said to be the *growth metric tensor*. As pointed out in [59], $\boldsymbol{C}_\gamma$ induces a Levi-Civita connection with non-trivial curvature [40, 41]. To see this, we first construct the Christoffel symbols of the connection, which, for a given coordinate system, are given by [61]

$$\Gamma^A{}_{MN} = \frac{1}{2}(\boldsymbol{C}_\gamma^{-1})^{AB}\left[\frac{\partial(\boldsymbol{C}_\gamma)_{BN}}{\partial X^M} + \frac{\partial(\boldsymbol{C}_\gamma)_{BM}}{\partial X^N} - \frac{\partial(\boldsymbol{C}_\gamma)_{MN}}{\partial X^B}\right], \tag{2}$$

and are symmetric in the lower indices, thereby implying the vanishing of the torsion [61], i.e.,

$$\mathbf{Tor} = (\Gamma^{A}_{\ MN} - \Gamma^{A}_{\ NM})\boldsymbol{E}_A \otimes \boldsymbol{E}^M \otimes \boldsymbol{E}^N = \mathbf{0}. \tag{3}$$

Then, we compute the fourth-order curvature tensor generated by $\boldsymbol{C}_\gamma$, i.e., $\boldsymbol{\mathcal{R}} = \mathcal{R}^{A}_{\ BMN}\boldsymbol{E}_A \otimes \boldsymbol{E}^B \otimes \boldsymbol{E}^M \otimes \boldsymbol{E}^N$, whose components read [40, 41, 61]

$$\mathcal{R}^{A}_{\ BMN} = \frac{\partial \Gamma^{A}_{\ BN}}{\partial X^M} - \frac{\partial \Gamma^{A}_{\ BM}}{\partial X^N} + \Gamma^{A}_{\ MD}\Gamma^{D}_{\ BN} - \Gamma^{A}_{\ ND}\Gamma^{D}_{\ BM}. \tag{4}$$

Moreover, by contracting the first and the third index of $\boldsymbol{\mathcal{R}}$, we obtain the Ricci curvature tensor,

$$\boldsymbol{R} = R_{BN}\boldsymbol{E}^B \otimes \boldsymbol{E}^N = \mathcal{R}^{D}_{\ BDN}\boldsymbol{E}^B \otimes \boldsymbol{E}^N, \tag{5}$$

and, by double-contracting $\boldsymbol{R}$ with $\boldsymbol{C}_\gamma^{-1}$, we determine the scalar curvature associated with growth, i.e.,

$$\kappa_\gamma = \boldsymbol{R} : \boldsymbol{C}_\gamma^{-1}. \tag{6}$$

3. A model of tumour growth

We report on a mathematical model of tumour growth that, in spite of two important differences, largely follows the path designated in [54]. The first difference concerns the benchmark problem that we solve, whose geometry is much simpler than the one used therein. This choice is due to the fact that we are interested here in purely modelling issues The second difference, as anticipated in Sect. 1, concerns the definition of the source/sink term r_s.

3.1. Growth and balance laws

By adhering to the model of tumour growth developed in [54], we describe a tumour in avascular stage as a biphasic medium comprising a solid and a fluid phase. At each point of the tissue, the amount of solid is measured by means of the apparent mass density $\varphi_\mathrm{s}\varrho_\mathrm{s}$, where φ_s and ϱ_s are said to be solid volumetric fraction and true mass density, respectively. Analogously, the amount of fluid is determined by the apparent density $\varphi_\mathrm{f}\varrho_\mathrm{f}$, with φ_f and ϱ_f being the volumetric fraction and true mass density, respectively. We recall that the *true* mass density of one of the phases constituting a mixture is the *intrinsic* mass density of the considered phase. In other words, it is the density that the phase would have if it were present in the mixture with unitary volumetric fraction. For this reason, the true mass density of a phase expresses its mass per unit volume of the phase itself, whereas the apparent

mass density expresses the phase mass per unit volume of the mixture as a whole.

Within our biphasic model, the tumour represents a saturated porous medium, so that the condition $\varphi_\mathrm{f} = 1 - \varphi_\mathrm{s}$ applies. Moreover, the fluid is assumed to feature only two constituents: nutrients, with mass fraction ω_N, and "water", with mass fraction $\omega_\mathrm{w} = 1 - \omega_\mathrm{N}$. We hypothesise that ω_N is very small, so that the mass density of the fluid, ϱ_f, can be regarded as constant, and approximately equal to the mass density of water. What we call "water" here is, in fact, a fluid comprising several substances, among which the constituents of the dead cells that return to the fluid in order to be expelled.

For simplicity, we prescribe that the solid phase consists of two types of cells only: the proliferating cells, with mass fraction ω_p, and the necrotic cells, with mass fraction $\omega_\mathrm{n} = 1 - \omega_\mathrm{p}$. The former ones describe the gain of mass of the tissue in response to the consumption of the nutrients. However, they become necrotic when the nutrients fall below a given threshold. The necrotic cells, in turn, are absorbed by the fluid, thereby accounting for the tissue's loss of mass due to cell death. In our model, the transition of a cell from the proliferating to the necrotic stage preserves the mass density of the cells. Hence, ϱ_s is independent of the composition of the solid phase, and may be regarded as constant, in spite of the fact that the mass fractions of the solid constituents may change in space and time [12, 54, 57].

To account for the gain and loss of mass pertaining to the proliferating and necrotic cells, we introduce their mass balance laws, which we write under the hypothesis that both types of cells move with the same velocity $\boldsymbol{v}_\mathrm{s}$, i.e., the solid phase velocity. By extending the model developed in [54], we write such balance laws as

$$\partial_t(\varphi_\mathrm{s}\varrho_\mathrm{s}\omega_\mathrm{p}) + \operatorname{div}(\varphi_\mathrm{s}\varrho_\mathrm{s}\omega_\mathrm{p}\boldsymbol{v}_\mathrm{s}) = r_\mathrm{pn} + r_\mathrm{fp} + r_{\mathrm{p}\gamma}, \tag{7a}$$

$$\partial_t(\varphi_\mathrm{s}\varrho_\mathrm{s}\omega_\mathrm{n}) + \operatorname{div}(\varphi_\mathrm{s}\varrho_\mathrm{s}\omega_\mathrm{n}\boldsymbol{v}_\mathrm{s}) = r_\mathrm{np} + r_\mathrm{nf} + r_{\mathrm{n}\gamma}, \tag{7b}$$

where r_pn, r_fp, r_np, r_nf, $r_{\mathrm{p}\gamma}$, and $r_{\mathrm{n}\gamma}$ denote the rates of mass uptake or depletion for the solid constituents. In particular, r_pn describes the portion of proliferating cells that, per unit volume and unit time, is converted into necrotic cells. In turn, r_np is the rate at which the necrotic cells are generated at the expenses of the proliferating ones, so that the condition $r_\mathrm{pn} + r_\mathrm{np} = 0$ is respected. Moreover, r_fp measures the growth of the proliferating cells due to the presence of nutrients, while r_nf represents the depletion of the necrotic cells in the fluid. We remark that r_pn, r_fp, r_np, and r_nf address processes that are at the basis of tumour evolution and, in this respect, their physical interpretation is rather intuitive. On the contrary, $r_{\mathrm{p}\gamma}$ and $r_{\mathrm{n}\gamma}$ are

introduced to investigate possible consequences of the properties of $\boldsymbol{F}_\gamma$ on growth itself. In other words, their task is to establish a feed-back loop among growth, the distortions that it generates, i.e., $\boldsymbol{F}_\gamma$, and the influence of those on the mass exchange terms. To the best of our knowledge, the presence of $r_{\mathrm{p}\gamma}$ and $r_{\mathrm{n}\gamma}$ in (7a) and (7b) is a novelty in the framework of mathematical modelling of tumour growth.

Since the mass fraction of the necrotic cells can be written as $\omega_{\mathrm{n}} = 1-\omega_{\mathrm{p}}$, Equation (7b) can be replaced by the mass balance law of the solid phase as a whole. Indeed, by adding together (7a) and (7b), we obtain [54]

$$\partial_t(\varphi_{\mathrm{s}}\varrho_{\mathrm{s}}\omega_{\mathrm{p}}) + \mathrm{div}(\varphi_{\mathrm{s}}\varrho_{\mathrm{s}}\omega_{\mathrm{p}}\boldsymbol{v}_{\mathrm{s}}) = r_{\mathrm{pn}} + r_{\mathrm{fp}} + r_{\mathrm{p}\gamma}, \tag{8a}$$

$$\partial_t(\varphi_{\mathrm{s}}\varrho_{\mathrm{s}}) + \mathrm{div}(\varphi_{\mathrm{s}}\varrho_{\mathrm{s}}\boldsymbol{v}_{\mathrm{s}}) = r_{\mathrm{s}}, \tag{8b}$$

where $r_{\mathrm{s}} = r_{\mathrm{fp}} + r_{\mathrm{nf}} + r_{\mathrm{p}\gamma} + r_{\mathrm{n}\gamma}$ is the overall source/sink of mass for the solid phase. In general, this term can be diverted into changes either of density or of volume. In this work, since ϱ_{s} is constant, r_{s} is diverted into changes of volume. To show this, we perform the backward Piola transformation of (8a) and (8b) by multiplying both equations by $J = \det \boldsymbol{F}$. Then, by splitting J as $J = J_{\mathrm{e}}J_\gamma$, with $J_{\mathrm{e}} = \det \boldsymbol{F}_{\mathrm{e}}$ and $J_\gamma = \det \boldsymbol{F}_\gamma$, we obtain

$$J_\gamma \Phi_{\mathrm{s}\nu}\varrho_{\mathrm{s}}\dot{\omega}_{\mathrm{p}} = J[r_{\mathrm{pn}} + r_{\mathrm{fp}}\ r_{\mathrm{p}\gamma} - \omega_{\mathrm{p}}r_{\mathrm{s}}], \tag{9a}$$

$$\dot{\overline{(J_\gamma \Phi_{\mathrm{s}\nu}\varrho_{\mathrm{s}})}} = Jr_{\mathrm{s}} = J[r_{\mathrm{fp}} + r_{\mathrm{nf}} + r_{\mathrm{p}\gamma} + r_{\mathrm{n}\gamma}], \tag{9b}$$

where $\Phi_{\mathrm{s}\nu} := J_{\mathrm{e}}\varphi_{\mathrm{s}}$ is the volumetric fraction of the solid phase expressed per unit volume of the intermediate, stress-free configuration. We require now that $\Phi_{\mathrm{s}\nu}$ is constant in time. Since ϱ_{s} is constant too, the left-hand-side of (9b) is proportional to $\dot{J}_\gamma = J_\gamma \mathrm{tr}[\dot{\boldsymbol{F}}_\gamma \boldsymbol{F}_\gamma^{-1}]$. Hence, (9a) and (9b) become

$$\dot{\omega}_{\mathrm{p}} = \frac{J[r_{\mathrm{pn}} + r_{\mathrm{fp}} + r_{\mathrm{p}\gamma} - \omega_{\mathrm{p}}r_{\mathrm{s}}]}{J_\gamma \Phi_{\mathrm{s}\nu}\varrho_{\mathrm{s}}}, \tag{10a}$$

$$\mathrm{tr}[\dot{\boldsymbol{F}}_\gamma \boldsymbol{F}_\gamma^{-1}] = \frac{J[r_{\mathrm{fp}} + r_{\mathrm{nf}} + r_{\mathrm{p}\gamma} + r_{\mathrm{n}\gamma}]}{\Phi_{\mathrm{s}\nu}\varrho_{\mathrm{s}}J_\gamma}. \tag{10b}$$

In general, besides varying the mass of a tissue, growth may also induce isochoric distortions. Accordingly, $\boldsymbol{F}_\gamma$ can be written as $\boldsymbol{F}_\gamma = [\det \boldsymbol{F}_\gamma]^{1/3}\bar{\boldsymbol{F}}_\gamma$, where $[\det \boldsymbol{F}_\gamma]^{1/3}$ measures the tissue's volume changes, and $\bar{\boldsymbol{F}}_\gamma$ is a volume-preserving tensor field that keeps track of the tissue's remodelling at constant mass. Thus, by adopting the notation $\gamma \equiv [\det \boldsymbol{F}_\gamma]^{1/3}$, we obtain [54]

$$\dot{\omega}_{\mathrm{p}} = \frac{J[r_{\mathrm{pn}} + r_{\mathrm{fp}} + r_{\mathrm{p}\gamma} - \omega_{\mathrm{p}}r_{\mathrm{s}}]}{J_\gamma \Phi_{\mathrm{s}\nu}\varrho_{\mathrm{s}}}, \tag{11a}$$

$$\frac{\dot{\gamma}}{\gamma} = \frac{J[r_{\mathrm{fp}} + r_{\mathrm{nf}} + r_{\mathrm{p}\gamma} + r_{\mathrm{n}\gamma}]}{3\Phi_{\mathrm{s}\nu}\varrho_{\mathrm{s}}J_{\gamma}}. \tag{11b}$$

Remark 2. *The hypothesis of constant true mass density of the solid phase is due to the fact that such phase is considered to be a representation of the tissue's cells. These, in turn, are essentially made of water, whose mass density is constant in the biophysical range relevant to our work. It follows, thus, that also* ϱ_{s} *can be safely assumed to be constant. However, if this assumption is relaxed, Eq.* (8b) *can be recast in the form*

$$\dot{\overline{\varphi_{\mathrm{s}}\varrho_{\mathrm{s}}}} + \varphi_{\mathrm{s}}\varrho_{\mathrm{s}}\mathrm{div}\boldsymbol{v}_{\mathrm{s}} = r_{\mathrm{s}}, \tag{12}$$

and, by exploiting the identity $\dot{J} = J(\mathrm{div}\boldsymbol{v}_{\mathrm{s}})$*, one can write*

$$J\dot{\varphi}_{\mathrm{s}}\varrho_{\mathrm{s}} + J\varphi_{\mathrm{s}}\dot{\varrho}_{\mathrm{s}} + \dot{J}\varphi_{\mathrm{s}}\varrho_{\mathrm{s}} = Jr_{\mathrm{s}}. \tag{13}$$

Since it holds that $\dot{J} = \dot{J}_{\mathrm{e}}J_{\mathrm{g}} + J_{\mathrm{e}}\dot{J}_{\gamma} = J\mathrm{tr}[\boldsymbol{L}_{\mathrm{e}}] + J\mathrm{tr}[\boldsymbol{L}_{\gamma}]$*, with* $\boldsymbol{L}_{\mathrm{e}} = \dot{\boldsymbol{F}}_{\mathrm{e}}\boldsymbol{F}_{\mathrm{e}}^{-1}$ *and* $\boldsymbol{L}_{\gamma} = \dot{\boldsymbol{F}}_{\gamma}\boldsymbol{F}_{\gamma}^{-1}$*, one obtains*

$$J\dot{\varphi}_{\mathrm{s}}\varrho_{\mathrm{s}} + J\varphi_{\mathrm{s}}\dot{\varrho}_{\mathrm{s}} + J\varphi_{\mathrm{s}}\varrho_{\mathrm{s}}\mathrm{tr}[\boldsymbol{L}_{\mathrm{e}}] + J\varphi_{\mathrm{s}}\varrho_{\mathrm{s}}\mathrm{tr}[\boldsymbol{L}_{\gamma}] = Jr_{\mathrm{s}}. \tag{14}$$

Moreover, we require $\mathrm{tr}[\boldsymbol{L}_{\gamma}] = r_{\mathrm{s}}/(\varphi_{\mathrm{s}}\varrho_{\mathrm{s}})$*, so that* (14) *becomes*

$$\dot{\varphi}_{\mathrm{s}}\varrho_{\mathrm{s}} + \varphi_{\mathrm{s}}\dot{\varrho}_{\mathrm{s}} + \varphi_{\mathrm{s}}\varrho_{\mathrm{s}}\mathrm{tr}[\boldsymbol{L}_{\mathrm{e}}] = 0, \tag{15}$$

which can be equivalently rearranged as $\dot{\overline{J_{\mathrm{e}}\varphi_{\mathrm{s}}\varrho_{\mathrm{s}}}} = 0$*. Thus, only the product* $\varphi_{\mathrm{s}}\varrho_{\mathrm{s}}$*, which individuates the mass density of the solid phase, is constant in time. Without loss of generality, it can be expressed with respect to the natural state, i.e., for* $J_{\mathrm{e}} = 1$*, as*

$$J_{\mathrm{e}}\varphi_{\mathrm{s}}\varrho_{\mathrm{s}} = \Phi_{\mathrm{s}\nu}\varrho_{\mathrm{s}0}, \tag{16}$$

where $\Phi_{\mathrm{s}\nu}$ *is the volumetric fraction in the natural state, and* $\varrho_{\mathrm{s}0}$ *denotes a constant reference value of the solid phase mass density. Equation* (16) *implies that* $\varphi_{\mathrm{s}}\varrho_{\mathrm{s}}$ *is a function of the elastic part of the overall deformation gradient tensor through* J_{e}*. In this case,* ϱ_{s} *can be either treated as an independent variable of the theory or specified through a state law. If the first option is chosen, the model necessitates an additional equation determining the volumetric fraction (cf. e.g. [62, 63, 64]). If, instead, the second choice is made, and one assumes that* ϱ_{s} *is a constitutive function e.g. of the com-*

position of the solid phase, one obtains

$$\varphi_{\mathrm{s}} = \frac{\Phi_{\mathrm{s}\nu}\hat{\varrho}_{\mathrm{s}}(\omega_{\mathrm{p}0})}{J_{\mathrm{e}}\hat{\varrho}_{\mathrm{s}}(\omega_{\mathrm{p}})} = \frac{J_{\gamma}\Phi_{\mathrm{s}\nu}\hat{\varrho}_{\mathrm{s}}(\omega_{\mathrm{p}0})}{J\hat{\varrho}_{\mathrm{s}}(\omega_{\mathrm{p}})}. \tag{17}$$

Here, $\hat{\varrho}_{\mathrm{s}}(\omega_{\mathrm{p}})$ is the constitutive representation of the true mass density of the solid phase. As anticipated above, it is specified as a function of the composition of the solid phase, which, within our model, is determined by the amount of proliferant and necrotic cells. Since it holds that $\omega_{\mathrm{p}} + \omega_{\mathrm{n}} = 1$, it suffices to use only one of the two mass fractions ω_{p} and ω_{n} to charaterise the composition. Upon choosing ω_{p}, we let $\hat{\varrho}_{\mathrm{s}}$ depend on ω_{p} only, and we take $\omega_{\mathrm{p}0}$ as a reference value for ω_{p}.

In conjunction with (11a) and (11b), also the mass balance laws of the nutrients and the fluid phase as a whole need to be studied

$$\partial_t(\varphi_{\mathrm{f}}\varrho_{\mathrm{f}}\omega_{\mathrm{N}}) + \mathrm{div}(\varphi_{\mathrm{f}}\varrho_{\mathrm{f}}\omega_{\mathrm{N}}\boldsymbol{v}_{\mathrm{f}} + \boldsymbol{y}_{\mathrm{N}}) = r_{\mathrm{Np}}, \tag{18a}$$

$$\partial_t(\varphi_{\mathrm{f}}\varrho_{\mathrm{f}}) + \mathrm{div}(\varphi_{\mathrm{f}}\varrho_{\mathrm{f}}\boldsymbol{v}_{\mathrm{f}}) = -r_{\mathrm{s}}. \tag{18b}$$

In (18a) and (18b), $\boldsymbol{v}_{\mathrm{f}}$ is the velocity of the fluid, $\boldsymbol{y}_{\mathrm{N}}$ is the mass flux vector associated with the motion of the nutrients relative to the fluid phase, and r_{Np} is the rate at which the nutrients are "eaten" by the proliferating cells. We remark that, to ensure the conservation of the mass of the biphasic medium under study, the right-hand-side of (18b) is taken equal to the negative of r_{s}.

After some calculations, (18a) and (18b) can be rephrased as

$$\varphi_{\mathrm{f}}\varrho_{\mathrm{f}}\dot{\omega}_{\mathrm{N}} + \varrho_{\mathrm{f}}\boldsymbol{q}\,\mathrm{grad}\omega_{\mathrm{N}} + \mathrm{div}\boldsymbol{y}_{\mathrm{N}} = r_{\mathrm{Np}} + \omega_{\mathrm{N}}r_{\mathrm{s}}, \tag{19a}$$

$$\mathrm{div}\,\boldsymbol{q} + \mathrm{div}\,\boldsymbol{v}_{\mathrm{s}} = \left(\frac{1}{\varrho_{\mathrm{s}}} - \frac{1}{\varrho_{\mathrm{f}}}\right) r_{\mathrm{s}}, \tag{19b}$$

where $\boldsymbol{q} = \varphi_{\mathrm{f}}[\boldsymbol{v}_{\mathrm{f}} - \boldsymbol{v}_{\mathrm{s}}]$ is said to be filtration velocity. Finally, (19a) and (19b) can be pulled-back to the reference configuration, thereby obtaining

$$(J - J_{\mathrm{g}}\Phi_{\mathrm{s}\nu})\varrho_{\mathrm{f}}\dot{\omega}_{\mathrm{N}} + \varrho_{\mathrm{f}}\boldsymbol{Q}\,\mathrm{Grad}\,\omega_{\mathrm{N}} + \mathrm{Div}\boldsymbol{Y}_{\mathrm{N}} = J[r_{\mathrm{Np}} + \omega_{\mathrm{N}}r_{\mathrm{s}}], \tag{20a}$$

$$\mathrm{Div}\,\boldsymbol{Q} + \dot{J} = \left(\frac{1}{\varrho_{\mathrm{s}}} - \frac{1}{\varrho_{\mathrm{f}}}\right) J r_{\mathrm{s}}, \tag{20b}$$

where $\boldsymbol{Q} = J\boldsymbol{F}^{-1}\boldsymbol{q}$ is the material filtration velocity, and $\boldsymbol{Y}_{\mathrm{N}} = J\boldsymbol{F}^{-1}\boldsymbol{y}_{\mathrm{N}}$ is the material mass flux vector of the nutrients. Under the hypothesis of validity of Darcy's law for the fluid, and of Fick's law for the nutrients, $\boldsymbol{Q}$ and $\boldsymbol{Y}_{\mathrm{N}}$ read $\boldsymbol{Q} = -\boldsymbol{K}\mathrm{Grad}\,p$ and $\boldsymbol{Y}_{\mathrm{N}} = -\varrho_{\mathrm{f}}\boldsymbol{D}\mathrm{Grad}\,\omega_{\mathrm{N}}$, with $\boldsymbol{K} = J\boldsymbol{F}^{-1}\boldsymbol{k}\boldsymbol{F}^{-\mathrm{T}}$ being the material permeability, p the pore pressure, and $\boldsymbol{D} = J\boldsymbol{F}^{-1}\boldsymbol{d}\boldsymbol{F}^{-\mathrm{T}}$

the material diffusivity tensor of the nutrients in water. The tensors $\boldsymbol{K}$ and $\boldsymbol{D}$ are the backward Piola transforms of the spatial permeability, $\boldsymbol{k}$, and of the spatial diffusivity, $\boldsymbol{d}$, respectively.

To conclude, we introduce the momentum balance law for the biphasic medium as a whole, which we write directly in material form (see [54] for details), i.e.,

$$\mathrm{Div}\left(-Jp\,\boldsymbol{g}^{-1}\boldsymbol{F}^{-\mathrm{T}}+\boldsymbol{P}_{\mathrm{sc}}\right)=\boldsymbol{0}, \tag{21}$$

where $\boldsymbol{P}_{\mathrm{sc}}$ is referred to as the constitutive part of the first Piola-Kirchhoff stress tensor of the solid phase.

3.2. Constitutive laws

In this work, the tumour tissue is assumed to be isotropic, and, for simplicity, $\boldsymbol{k}$ and $\boldsymbol{d}$ are taken "*unconditionally isotropic*" [65], which means that they are both proportional to the inverse metric tensor $\boldsymbol{g}^{-1}$. Hence, we write $\boldsymbol{k}=k_0\boldsymbol{g}^{-1}$ and $\boldsymbol{d}=d_0\boldsymbol{g}^{-1}$, where k_0 is given in the form of the Holmes-Mow scalar permeability [65, 66], and d_0 is defined as a function of J and J_γ through the fluid phase volumetric fraction, i.e.,

$$\begin{aligned} k_0 &= k_{0\mathrm{R}}\left[\frac{\Phi_{\mathrm{s}\nu}\varphi_{\mathrm{f}}}{\varphi_{\mathrm{f}0}\varphi_{\mathrm{s}}}\right]^{m_0}\exp\left(\frac{m_1}{2}\left[\frac{J^2-J_\gamma^2}{J_\gamma^2}\right]\right)\\ &= k_{0\mathrm{R}}\left[\frac{J-J_\gamma\Phi_{\mathrm{s}\nu}}{J_\gamma\varphi_{\mathrm{f}0}}\right]^{m_0}\exp\left(\frac{m_1}{2}\left[\frac{J^2-J_\gamma^2}{J_\gamma^2}\right]\right), \end{aligned} \tag{22a}$$

$$d_0=\varphi_{\mathrm{f}}d_{0\mathrm{R}}=\frac{J-J_\gamma\Phi_{\mathrm{s}\nu}}{J}d_{0\mathrm{R}}. \tag{22b}$$

In (22a), $\varphi_{\mathrm{f}0}=1-\Phi_{\mathrm{s}\nu}$ is a reference value of the fluid phase volumetric fraction, m_0 and m_1 are constant material coefficients, and $k_{0\mathrm{R}}$ is said to be the reference permeability of the medium. This quantity is assumed to be a constant in this work, even though it should be defined as a function of material points in a more general setting. The factor $d_{0\mathrm{R}}$ in (22b) is the reference diffusivity, which, for simplicity, is assumed here to be constant. This condition, in fact, may be violated when the nutrient mass fraction, ω_{N}, is sufficiently greater than zero, in which case $d_{0\mathrm{R}}$ should be defined as a function of ω_{N}.

By substituting (22a) and (22b) into the definitions of $\boldsymbol{k}$ and $\boldsymbol{d}$, and the corresponding results into the expressions of the material permeability and diffusivity, we find

$$\boldsymbol{K}=Jk_0\boldsymbol{C}^{-1}, \tag{23a}$$

$$\boldsymbol{D}=(J-J_\gamma\Phi_{\mathrm{s}\nu})d_{0\mathrm{R}}\boldsymbol{C}^{-1}. \tag{23b}$$

Besides being isotropic, the solid phase of the tissue is assumed to be hyperelastic. Hence, its mechanical behaviour can be described by means of a strain energy density function, $\mathcal{W}$, which we express per unit volume of the reference configuration. To account for the variation of internal structure induced by growth, $\mathcal{W}$ is given in terms of a constitutive function, $\tilde{\mathcal{W}}$, of $\boldsymbol{F}$, $\boldsymbol{F}_\gamma$, and material points, X. The purely elastic contribution of the material to the overall energy can be measured by introducing the energy density $\mathcal{W}_\nu$, defined per unit volume of the stress-free configuration, whose associated constitutive representation, $\tilde{\mathcal{W}}_\nu$, depends on $\boldsymbol{F}$ and $\boldsymbol{F}_\gamma$ exclusively through $\boldsymbol{F}_\mathrm{e}$. Hence, we write [28] (see also [67] for details)

$$\mathcal{W} = J_\gamma \mathcal{W}_\nu, \quad \tilde{\mathcal{W}}(\boldsymbol{F}, \boldsymbol{F}_\gamma, X) = J_\gamma \tilde{\mathcal{W}}_\nu(\boldsymbol{F}_\mathrm{e}). \tag{24}$$

For $\tilde{\mathcal{W}}_\nu(\boldsymbol{F}_\mathrm{e})$, we choose a constitutive law of the Holmes-Mow type [66], i.e.,

$$\begin{aligned}
\tilde{\mathcal{W}}_\nu(\boldsymbol{F}_\mathrm{e}) &= \hat{\mathcal{W}}_\nu(\boldsymbol{C}_\mathrm{e}) = \check{\mathcal{W}}_\nu(\hat{I}_1(\boldsymbol{C}_\mathrm{e}), \hat{I}_2(\boldsymbol{C}_\mathrm{e}), \hat{I}_3(\boldsymbol{C}_\mathrm{e})) \\
&= \alpha_0 \left\{ \exp(\hat{\Psi}(\boldsymbol{C}_\mathrm{e})) - 1 \right\}, \qquad (25a) \\
\hat{\Psi}(\boldsymbol{C}_\mathrm{e}) &= \check{\Psi}(\hat{I}_1(\boldsymbol{C}_\mathrm{e}), \hat{I}_2(\boldsymbol{C}_\mathrm{e}), \hat{I}_3(\boldsymbol{C}_\mathrm{e})) \\
&= \alpha_1[\hat{I}_1(\boldsymbol{C}_\mathrm{e}) - 3] + \alpha_2[\hat{I}_2(\boldsymbol{C}_\mathrm{e}) - 3] - \alpha_3 \ln\Big(\hat{I}_3(\boldsymbol{C}_\mathrm{e})\Big), \qquad (25b)
\end{aligned}$$

where $\boldsymbol{C}_\mathrm{e} = \boldsymbol{F}_\mathrm{e}^\mathrm{T}.\boldsymbol{F}_\mathrm{e}$ is the elastic Cauchy-Green deformation tensor, $\hat{\mathcal{W}}_\nu(\boldsymbol{C}_\mathrm{e})$ is introduced to comply with objectivity, and, to account for isotropy, the dependence of $\check{\mathcal{W}}_\nu$ on $\boldsymbol{C}_\mathrm{e}$ is expressed through the principal invariants

$$\begin{aligned}
I_1 &= \hat{I}_1(\boldsymbol{C}_\mathrm{e}) = \mathrm{tr}\left(\boldsymbol{\eta}^{-1}\boldsymbol{C}_\mathrm{e}\right), \qquad (26a) \\
I_2 &= \hat{I}_2(\boldsymbol{C}_\mathrm{e}) = \tfrac{1}{2}\{[\hat{I}_1(\boldsymbol{C}_\mathrm{e})]^2 - \mathrm{tr}[(\boldsymbol{\eta}^{-1}\boldsymbol{C}_\mathrm{e})^2]\}, \qquad (26b) \\
I_3 &= \hat{I}_3(\boldsymbol{C}_\mathrm{e}) = \det \boldsymbol{C}_\mathrm{e}. \qquad (26c)
\end{aligned}$$

Here, $\boldsymbol{\eta}$ is the metric tensor of the "intermediate configuration" and, by using the equality $\boldsymbol{C}_\mathrm{e} = \boldsymbol{F}_\gamma^{-\mathrm{T}} \boldsymbol{C} \boldsymbol{F}_\gamma^{-1}$, it can be eliminated from (26a)–(26c), so that the invariants can be rephrased as functions of $\boldsymbol{C}$ and $\boldsymbol{C}_\gamma$. Finally, in (25b), the material coefficients α_0, α_1, α_2, and α_3 are functions of Lamé's elastic parameters [68] (in particular, as in [66], we set $\alpha_3 = 1$), i.e.,

$$\alpha_0 = \frac{2\mu + \lambda}{4\alpha_3}, \quad \alpha_1 = \alpha_3 \frac{2\mu - \lambda}{2\mu + \lambda}, \quad \alpha_2 = \alpha_3 \frac{\lambda}{2\mu + \lambda}, \quad \alpha_3 = \alpha_1 + 2\alpha_2. \tag{27}$$

Equations (24), (25a), (25b), and (26a)–(26c) permit to calculate the consti-

tutive part of the second Piola-Kirchhoff stress tensor of the solid phase:

$$\begin{aligned}\boldsymbol{S}_{\mathrm{sc}} = \hat{\boldsymbol{S}}_{\mathrm{sc}}(\boldsymbol{C},\boldsymbol{C}_\gamma) &= \left[J_\gamma \boldsymbol{F}_\gamma^{-1}\left(2\frac{\partial \hat{\mathcal{W}}_\nu}{\partial \boldsymbol{C}_{\mathrm{e}}}(\boldsymbol{C}_{\mathrm{e}})\right)\boldsymbol{F}_\gamma^{-\mathrm{T}}\right] \\ &= 2J_\gamma b_1 \boldsymbol{C}_\gamma^{-1} + 2J_\gamma b_2[I_1\boldsymbol{C}_\gamma^{-1} - \boldsymbol{C}_\gamma^{-1}\boldsymbol{C}\boldsymbol{C}_\gamma^{-1}] + 2J_\gamma b_3 I_3 \boldsymbol{C}^{-1},\end{aligned} \tag{28}$$

with $b_i = \partial \check{\mathcal{W}}_\nu/\partial I_i$, $i \in \{1,2,3\}$. Consequently, the first Piola-Kirchhoff stress tensor $\boldsymbol{P}_{\mathrm{sc}}$ can be expressed constitutively as

$$\boldsymbol{P}_{\mathrm{sc}} = \hat{\boldsymbol{P}}_{\mathrm{sc}}(\boldsymbol{F},\boldsymbol{C}_\gamma) = \boldsymbol{F}\hat{\boldsymbol{S}}_{\mathrm{sc}}(\boldsymbol{C},\boldsymbol{C}_\gamma), \tag{29}$$

and, thus, the constitutive part of the Cauchy stress tensor reads

$$\begin{aligned}\boldsymbol{\sigma}_{\mathrm{sc}} = \hat{\boldsymbol{\sigma}}_{\mathrm{sc}}(\boldsymbol{F},\boldsymbol{C}_\gamma) &= J^{-1}\hat{\boldsymbol{P}}_{\mathrm{sc}}(\boldsymbol{F},\boldsymbol{C}_\gamma)\boldsymbol{F}^{\mathrm{T}} \\ &= \frac{J_\gamma}{J}\left\{2b_1\boldsymbol{b}_{\mathrm{e}} + 2b_2[I_1\boldsymbol{b}_{\mathrm{e}} - \boldsymbol{b}_{\mathrm{e}}.\boldsymbol{b}_{\mathrm{e}}] + 2b_3 I_3 \boldsymbol{g}^{-1}\right\},\end{aligned} \tag{30}$$

where $\boldsymbol{b}_{\mathrm{e}} = \boldsymbol{F}\boldsymbol{C}_\gamma^{-1}\boldsymbol{F}^{\mathrm{T}}$ is the elastic right Cauchy-Green deformation tensor.

3.3. Sources and sinks of mass

To model growth, it is necessary to describe the mass exchanges among the constituents of the system under study. In our framework, this requires to provide mathematical expressions for r_{fp}, r_{pn}, r_{nf}, and r_{Np}, and to relate each of these quantities with the appropriate set of chemo-mechanical variables. For r_{pn}, r_{nf}, r_{Np} and r_{fp}, we adopt the phenomenological expressions suggested in [54], which we report here with slight changes of notation, i.e.,

$$r_{\mathrm{pn}} = -\zeta_{\mathrm{pn}}\left\langle 1 - \frac{\omega_{\mathrm{N}}}{\omega_{\mathrm{Ncr}}}\right\rangle_+ \varphi_{\mathrm{s}}\omega_{\mathrm{p}} = -\zeta_{\mathrm{pn}}\left\langle 1 - \frac{\omega_{\mathrm{N}}}{\omega_{\mathrm{Ncr}}}\right\rangle_+ \frac{J_\gamma \Phi_{\mathrm{s}\nu}}{J}\omega_{\mathrm{p}}, \tag{31a}$$

$$r_{\mathrm{nf}} = -\zeta_{\mathrm{nf}}\varphi_{\mathrm{s}}[1-\omega_{\mathrm{p}}] = -\zeta_{\mathrm{nf}}\frac{J_\gamma\Phi_{\mathrm{s}\nu}}{J}[1-\omega_{\mathrm{p}}], \tag{31b}$$

$$r_{\mathrm{Np}} = -\zeta_{\mathrm{Np}}\frac{\omega_{\mathrm{N}}}{\omega_{\mathrm{N}}+\omega_{\mathrm{N0}}}\varphi_{\mathrm{s}}\omega_{\mathrm{p}} = -\zeta_{\mathrm{Np}}\frac{\omega_{\mathrm{N}}}{\omega_{\mathrm{N}}+\omega_{\mathrm{N0}}}\frac{J_\gamma\Phi_{\mathrm{s}\nu}}{J}\omega_{\mathrm{p}}, \tag{31c}$$

$$\begin{aligned} r_{\mathrm{fp}} &= \zeta_{\mathrm{fp}}\left\langle\frac{\omega_{\mathrm{N}}-\omega_{\mathrm{Ncr}}}{\omega_{\mathrm{Nenv}}-\omega_{\mathrm{Ncr}}}\right\rangle_+\left[1-\frac{\delta_1\langle\bar{\sigma}\rangle_+}{\delta_2+\langle\bar{\sigma}\rangle_+}\right]\frac{\varphi_{\mathrm{f}}\varphi_{\mathrm{s}}}{\varphi_{\mathrm{f0}}}\omega_{\mathrm{p}} \\ &= \zeta_{\mathrm{fp}}\left\langle\frac{\omega_{\mathrm{N}}-\omega_{\mathrm{Ncr}}}{\omega_{\mathrm{Nenv}}-\omega_{\mathrm{Ncr}}}\right\rangle_+\left[1-\frac{\delta_1\langle\bar{\sigma}\rangle_+}{\delta_2+\langle\bar{\sigma}\rangle_+}\right]\frac{J-J_\gamma\Phi_{\mathrm{s}\nu}}{J\varphi_{\mathrm{f0}}}\frac{J_\gamma\Phi_{\mathrm{s}\nu}}{J}\omega_{\mathrm{p}}.\end{aligned} \tag{31d}$$

The terms r_{pn}, r_{nf}, and r_{Np} are sinks of mass for the constituents to which they refer. In particular, r_{pn} represents the loss of mass of the proliferant cells that become necrotic. The term r_{fp}, instead, is a source of mass for

the proliferant cells, and represents the mass gained by this population of cells at the expenses of the fluid. We need to emphasise that both r_{pn} and r_{fp} represent processes whose occurrence is strongly controlled by the availability of the nutrients in the tissue. To describe mathematically the concept of "availability of the nutrients", we introduce a critical value of the nutrient mass fraction, $\omega_{\mathrm{Ncr}} \in \,]0,1[$, and we model the transfers of mass associated with r_{pn} and r_{fp} as threshold processes. Accordingly, when it holds that $\omega_{\mathrm{N}} \leq \omega_{\mathrm{Ncr}}$, the proliferant cells die, which means that r_{pn} is active, while r_{fp} is switched off. On the contrary, for $\omega_{\mathrm{N}} > \omega_{\mathrm{Ncr}}$, r_{pn} must vanish identically, whereas r_{fp} is switched on. Such activation and deactivation of r_{pn} and r_{fp} is formulated by means of the operator $\langle \cdot \rangle_+$, which returns the argument to which it is applied, when the argument is greater than zero, and zero otherwise. Thus, it is introduced to switch off cell death when the mass fraction of the nutrients, ω_{N}, is above, or equal to, the threshold level $\omega_{\mathrm{Ncr}} \in \,]0,1[$, which is assumed to be a constant of the model.

In our model, the coefficients ζ_{pn}, ζ_{nf}, ζ_{Np} and ζ_{fp} are constants, and can be related to the characteristic time scales with which, respectively, the proliferating cells die, the necrotic cells are converted into fluid, the nutrients are consumed and the interstitial fluid becomes a tumor due to cell growth.

We notice that the sinks defined in (31a)–(31d) depend on the solid phase volumetric fraction, $\varphi_{\mathrm{s}} = (J_\gamma \Phi_{\mathrm{s}\nu})/J$, in such a way that they vanish for vanishing φ_{s}. For the same reason, r_{pn} must be zero for zero ω_{p}, r_{Np} must be zero when ω_{p} or ω_{N} is zero, and r_{nf} must be zero for unitary ω_{p}, i.e., for zero ω_{n} (indeed, $\omega_{\mathrm{n}} = 1 - \omega_{\mathrm{p}}$). We remark, in addition, that the dependence of r_{Np} on ω_{N} is taken from Population Dynamics [69], with the constant $\omega_{\mathrm{N0}} \in \,]0,1]$ being a reference value of the nutrient concentration, introduced to modulate the rate at which their uptake occurs. The dependence of r_{fp} on φ_{s} and $\varphi_{\mathrm{f}} = 1 - \varphi_{\mathrm{s}}$ guarantees that growth ceases in the limit of compaction, i.e., when all the fluid flows away, and the porous medium features no voids, or when the solid disappears, which means that φ_{s} becomes zero. Besides, r_{fp} vanishes for vanishing ω_{p}, and is modulated by stress through the term $\langle \bar{\sigma} \rangle_+$, where $\bar{\sigma}$ is defined as

$$\bar{\sigma} = -\tfrac{1}{3}(\boldsymbol{g} : \boldsymbol{\sigma}_{\mathrm{sc}}) = -\frac{\frac{2}{3}\sum_{i=1}^{3} i\, b_i I_i}{J_{\mathrm{e}}}. \tag{32}$$

We reserve now a separate treatment for the non-standard terms $r_{\mathrm{p}\gamma}$ and $r_{\mathrm{n}\gamma}$. In particular, for the sake of simplicity, we set $r_{\mathrm{n}\gamma} = 0$ and we prescribe $r_{\mathrm{p}\gamma}$ as

$$r_{\mathrm{p}\gamma} = c\left[\zeta_{\mathrm{fp}} \frac{\omega_{\mathrm{N}}}{\omega_{\mathrm{Ncr}}} \frac{\varphi_{\mathrm{f}}\varphi_{\mathrm{s}}}{\varphi_{\mathrm{f0}}} \omega_{\mathrm{p}}\right] \kappa_\gamma = c\left[\zeta_{\mathrm{fp}} \frac{\omega_{\mathrm{N}}}{\omega_{\mathrm{Ncr}}} \frac{J - J_\gamma \Phi_{\mathrm{s}\nu}}{J\varphi_{\mathrm{f0}}} \frac{J_\gamma \Phi_{\mathrm{s}\nu}}{J} \omega_{\mathrm{p}}\right] \kappa_\gamma. \tag{33}$$

With the formulation of $r_{\mathrm{p}\gamma}$ given in (33), we assume that $r_{\mathrm{p}\gamma}$ is proportional to κ_γ through the factor $c\,\zeta_{\mathrm{fp}}(\omega_{\mathrm{N}}/\omega_{\mathrm{Ncr}})(\varphi_{\mathrm{f}}\varrho_{\mathrm{s}})/\varphi_{\mathrm{f0}}$. In this work, the product $c\,\zeta_{\mathrm{fp}}$ is assumed to be constant and it represents, with respect to a suitable time scale, the way in which the inhomogeneities induced by growth evolve in the tissue. Moreover, as explained above for the standard terms (31a)–(31d), we need to account for the limit cases in which compaction occurs ($\varphi_{\mathrm{f}} = 0$) or the solid phase is locally absent ($\varphi_{\mathrm{s}} = 0$). In fact, we ensure that $r_{\mathrm{p}\gamma}$ vanishes when φ_{f} or φ_{s} vanish. Finally, we relate the availability of nutrients to growth. In fact, we prescribe that growth does not take place if $\omega_{\mathrm{N}} = 0$, and we modulate the growth rate through the reference value ω_{Ncr}. This factor, indeed, is introduced to re-scale the current mass fraction of the nutrients, ω_{N}. In particular, the effect of κ_γ is amplified for $\omega_{\mathrm{N}} > \omega_{\mathrm{Ncr}}$, and reduced for $\omega_{\mathrm{N}} \leq \omega_{\mathrm{Ncr}}$.

For the sake of a lighter exposition, in the present work we suppress the rotations related to growth, so that $\boldsymbol{R}_\gamma$ reduces to a shifter [61] from $T\mathscr{B}$ to $T\mathscr{N}_t$, and we assume that $\boldsymbol{U}_\gamma$ represents a pure dilatation, i.e., we set $\boldsymbol{U}_\gamma = \gamma\boldsymbol{I}$. This form of $\boldsymbol{U}_\gamma$ also implies $J_\gamma = \gamma^3$ and $\boldsymbol{C}_\gamma = \gamma^2\boldsymbol{G}$, so that the material metric, $\boldsymbol{G}$, is rescaled by γ^2. Hence, no remodelling is considered in this work, and growth is entirely expressed in terms of an evolution law for γ, which, for given r_{fp} and r_{nf}, coincides with (11b).

We emphasise that the introduction of κ_γ in our model of tumour growth is the major novelty of our work, and it constitutes the principal difference with respect to the model developed in [54]. The difference is in the fact that, while (11b) is an ordinary differential equation in [54], it is a partial differential equation in our model. This feature of our approach allows for an explicit resolution of the spatial variability of γ and, more importantly, it permits to estimate to what extent such variability influences growth. In fact, going through the calculations leading to (6), we notice that κ_γ features the derivatives of γ up to the second order. Hence, by introducing $r_{\mathrm{p}\gamma}$ into (11b), we obtain a nonlinear diffusion-reaction like equation in the unknown γ. Solving this equation shows how the resolved spatial variability of γ influences the evolution of the other model descriptors, i.e., the mass fraction of the proliferating cells, the mass fraction of the nutrients, the motion, and pressure.

Looking at (11b), and combining it with the definitions (31b), (31d), and (33), we notice that, when the mass fraction of the nutrients, ω_{N}, is below the threshold ω_{Ncr} (so that $r_{\mathrm{fp}} = 0$), we obtain

$$\frac{\dot{\gamma}}{\gamma} = c\left[\frac{\zeta_{\mathrm{fp}}}{3\varrho_{\mathrm{s}}}\frac{\omega_{\mathrm{N}}}{\omega_{\mathrm{Ncr}}}\frac{\varphi_{\mathrm{f}}}{\varphi_{\mathrm{f0}}}\omega_{\mathrm{p}}\right]\kappa_\gamma - \frac{\zeta_{\mathrm{nf}}}{3\varrho_{\mathrm{s}}}[1-\omega_{\mathrm{p}}]. \tag{34}$$

In (34), indeed, the evolution of γ is governed by an affine function of κ_γ, and is modulated by the mass fractions ω_p and ω_N. More generally, instead, when ω_N is above ω_Ncr, Equation (34) becomes:

$$\begin{aligned}\frac{\dot\gamma}{\gamma} =& c\left[\frac{\zeta_\mathrm{fp}}{3\varrho_\mathrm{s}}\frac{\omega_\mathrm{N}}{\omega_\mathrm{Ncr}}\frac{\varphi_\mathrm{f}}{\varphi_\mathrm{f0}}\omega_\mathrm{p}\right]\kappa_\gamma - \frac{\zeta_\mathrm{nf}}{3\varrho_\mathrm{s}}[1-\omega_\mathrm{p}] \\ &+ \frac{\zeta_\mathrm{fp}}{3\varrho_\mathrm{s}}\left\langle\frac{\omega_\mathrm{N}-\omega_\mathrm{Ncr}}{\omega_\mathrm{Nenv}-\omega_\mathrm{Ncr}}\right\rangle_+\left[1-\frac{\delta_1\langle\bar\sigma\rangle_+}{\delta_2+\langle\bar\sigma\rangle_+}\right]\frac{\varphi_\mathrm{f}}{\varphi_\mathrm{f0}}\omega_\mathrm{p}. \end{aligned} \tag{35}$$

Equation (35) combines two models: The first two terms on the right-hand-side of (35) are an adaptation of the model by Epstein [42] to our biphasic problem, which requires the introduction of the mass fraction of nutrients and proliferating cells as well as the volumetric fraction of the fluid phase. The last term, instead, is taken from the model by Mascheroni et al. [54] and has phenomenological nature in order to account for the fact that growth occurs when the mass fraction of the nutrients, ω_N, is greater than ω_Ncr, and it is modulated by stress.

Remark 3. *Following [42], one could formulate a more general model, without the* a priori *assumptions of no growth-induced rotations and $\boldsymbol{U}_\gamma = \gamma\boldsymbol{I}$. In this case, a possible evolution law for $\boldsymbol{F}_\gamma$ could be obtained by relating $\dot{\boldsymbol{F}}_\gamma$ to a known function of $\boldsymbol{\mathcal{R}}$ and* Grad$\boldsymbol{\mathcal{R}}$ *[42]. Such an evolution law, however, is out of the scope of this work. Therefore, for the moment, we simply neglect* Grad$\boldsymbol{\mathcal{R}}$ *in the evolution law for $\boldsymbol{F}_\gamma$, thereby keeping only its derivatives up to the second order. Moreover, since in our framework it holds that $\boldsymbol{U}_\gamma = \gamma\boldsymbol{I}$, we end up with model in which the evolution of γ is a function of the scalar curvature, κ_γ, whereas it does not depend on the spatial derivatives of γ of order higher than the second.*

4. Solution of a benchmark problem

4.1. Summary of the model

Before addressing the details of the considered benchmark problem, we summarise the model equations, and declare the unknowns to be determined. In doing this, we perform the following simplifications: (a) since the cells consist mainly of water, the mass densities ϱ_s and ϱ_f are regarded as equal to each other, so that the right-hand-side of (20a) is zero; (b) the advective term $\boldsymbol{Q}\,\mathrm{Grad}\,\omega_\mathrm{N}$ is considered to be negligible with respect to the other terms of (20a). In conclusion, the model equations are given by (11a), (11b), (20a), (20b), and (21), which we rewrite as

$$\mathrm{Div}\left[-Jp\boldsymbol{g}^{-1}\boldsymbol{F}^{-\mathrm{T}} + \boldsymbol{P}_\mathrm{sc}\right] = \boldsymbol{0}, \tag{36a}$$

$$\dot{J} - \mathrm{Div}\,[\boldsymbol{K}\mathrm{Grad}\,p] = 0, \tag{36b}$$

$$(J - \gamma^3\Phi_{\mathrm{s}\nu})\dot{\omega}_{\mathrm{N}} - \mathrm{Div}\,[\boldsymbol{D}\mathrm{Grad}\,\omega_{\mathrm{N}}] = J\left(\frac{r_{\mathrm{Np}}}{\varrho_{\mathrm{f}}} + \frac{3\gamma^3\,\Phi_{\mathrm{s}\nu}\,\omega_{\mathrm{N}}}{J}\frac{\dot{\gamma}}{\gamma}\right), \tag{36c}$$

$$\dot{\omega}_{\mathrm{p}} = -\frac{\zeta_{\mathrm{pn}}}{\varrho_{\mathrm{s}}}\left\langle 1 - \frac{\omega_{\mathrm{N}}}{\omega_{\mathrm{Ncr}}}\right\rangle_{+}\omega_{\mathrm{p}} + \frac{\zeta_{\mathrm{nf}}}{\varrho_{\mathrm{s}}}[1-\omega_{\mathrm{p}}] + 3[1-\omega_{\mathrm{p}}]\frac{\dot{\gamma}}{\gamma}, \tag{36d}$$

$$\frac{\dot{\gamma}}{\gamma} = c\left[\frac{\zeta_{\mathrm{fp}}}{3\varrho_{\mathrm{s}}}\frac{\omega_{\mathrm{N}}}{\omega_{\mathrm{Ncr}}}\frac{J-\gamma^3\Phi_{\mathrm{s}\nu}}{J-J\Phi_{\mathrm{s}\nu}}\omega_{\mathrm{p}}\right]\kappa_\gamma + \frac{J[r_{\mathrm{fp}}+r_{\mathrm{nf}}]}{3\gamma^3\Phi_{\mathrm{s}\nu}\varrho_{\mathrm{s}}}, \tag{36e}$$

where r_{nf}, r_{Np}, and r_{fp} are defined in (31b), (31c), and (31d). Consistently with (36a)–(36e), the unknown of the models are the motion of the solid phase, χ, the pressure, p, the nutrient mass fraction, ω_{N}, the growth parameter, γ, and the mass fraction of the proliferating cells, ω_{p}. Finally, $\boldsymbol{K}$, $\boldsymbol{D}$, and $\boldsymbol{P}_{\mathrm{sc}}$ are specified in (23a), (23b), and (29), and all the material parameters are reported in Table 1 and in Table 2.

4.2. Description of the benchmark test

As a proof of concept, we specialise now Equations (36a)–(36e) to a benchmark problem taken from the literature. For our purposes, we select the problem of "*isotropic and homogeneous growth inside a rigid cylinder*", formulated in [55] for the case of mono-phasic growing medium, and we adapt it to our scopes.

Also in our formulation, the growth is isotropic, i.e., $\boldsymbol{U}_\gamma = \gamma\boldsymbol{I}$, and takes place inside a tissue specimen of cylindrical shape, with undeformable curved surface. Hence, both the reference and the current configurations of the tissue have cylindrical shapes, with equal radius and different lengths. We indicate by R_{in} and L the initial radius and the initial length of the cylinder, respectively. Moreover, the reference configuration is covered with a system of cylindrical coordinates $\hat{X} = (R, \Theta, Z)$, where R, Θ, and Z are the radial, circumferential, and axial coordinate, respectively. Analogously, the generic current configuration of the tissue is covered with the system of cylindrical coordinates $\hat{x} = (r, \vartheta, z)$. Any rigid rotation of the specimen about the axis of the cylinder is suppressed from the outset.

The restrictions imposed on χ imply that only the axial component of the momentum balance law (36a) has to be solved, and that the sole unknown component of the motion is the axial one, χ^z, while the radial and circumferential ones, χ^r and χ^ϑ, return the radial and the angular coordinate, respectively.

The growth cannot be assumed to be homogeneous in our framework, as the scalar curvature, κ_γ, would then be trivially zero, and our model would boil down to a simple biphasic rephrasing of the model presented in [55]. On

the contrary, to highlight the role of κ_γ, we prescribe initial distributions of γ with a strong gradient.

In [55], the two extremities of the considered cylinder are free of applied forces, so that the axial component of stress is zero both at two outermost sections of the cylinder and, because of homogeneity, everywhere else inside it. In our setting, however, we may only conclude that the overall axial Cauchy stress, $\sigma^{zz} = -p + \sigma_{\rm sc}^{zz}$ is zero, whereas the pressure, p, and the constitutive Cauchy stress, $\sigma_{\rm sc}^{zz}$, cannot be individually zero because of the point-dependent distribution of γ. In fact, they can be such only in the limit in which the initial inhomogeneities relax, and the conditions $p = 0$ and $\sigma_{\rm sc}^{zz} = 0$ are the unique, stationary solutions to (36a) and (36b). Further differences with [55] are due to the different constitutive relations which we work with, and to the fact that our solid phase consists of two types of cells.

To solve (36a)–(36e) compatibly with the descriptions given so far, we prescribe the reference configuration of the tissue, $\mathscr{B}$, to be of cylindrical shape, and we assign the following set of boundary conditions, which apply for all times:

$$
\begin{aligned}
&\chi^r = R_{\rm in}, && \text{on } (\partial\mathscr{B})_{\rm C}, && \text{(37a)}\\
&\chi^\vartheta = \Theta, && \text{on } (\partial\mathscr{B})_{\rm C}, && \text{(37b)}\\
&(-Jp\boldsymbol{g}^{-1}\boldsymbol{F}^{-\rm T} + \boldsymbol{P}_{\rm sc}).\boldsymbol{N}_{\rm A} = \boldsymbol{0}, && \text{on } (\partial\mathscr{B})_{\rm Left} \text{ and } (\partial\mathscr{B})_{\rm Right}, && \text{(37c)}\\
&(-\boldsymbol{K}{\rm Grad}\, p).\boldsymbol{N}_{\rm C} = 0, && \text{on } (\partial\mathscr{B})_{\rm C}, && \text{(37d)}\\
&p = 0, && \text{on } (\partial\mathscr{B})_{\rm Left} \text{ and } (\partial\mathscr{B})_{\rm Right}, && \text{(37e)}\\
&(-\varrho_{\rm f}\boldsymbol{D}{\rm Grad}\,\omega_{\rm N}).\boldsymbol{N}_{\rm C} = 0, && \text{on } (\partial\mathscr{B})_{\rm C}, && \text{(37f)}\\
&\omega_{\rm N} = \omega_{\rm Nenv}, && \text{on } (\partial\mathscr{B})_{\rm Left} \text{ and } (\partial\mathscr{B})_{\rm Right}, && \text{(37g)}\\
&({\rm Grad}\gamma)\boldsymbol{N} = 0, && \text{on } \partial\mathscr{B}. && \text{(37h)}
\end{aligned}
$$

In (37a)–(37g), $(\partial\mathscr{B})_{\rm C}$ is the lateral boundary of the cylindric specimen, whereas $(\partial\mathscr{B})_{\rm Left}$ and $(\partial\mathscr{B})_{\rm Right}$ are the left and the right surfaces at the extremities of $\mathscr{B}$, respectively, $\boldsymbol{N}_{\rm A}$ is the unit vector field normal to $(\partial\mathscr{B})_{\rm Left}$ and $(\partial\mathscr{B})_{\rm Right}$, $\boldsymbol{N}_{\rm C}$ is the unit vector field oriented normal to $(\partial\mathscr{B})_{\rm C}$, and $R_{\rm in}$ is the initial radius of the cylinder. Furthermore, it holds that $\partial\mathscr{B} = (\partial\mathscr{B})_{\rm Left} \cup (\partial\mathscr{B})_{\rm Right} \cup (\partial\mathscr{B})_{\rm C}$, and that $\boldsymbol{N}$ is the unit vector field normal to $\partial\mathscr{B}$.

Before going further, we remark that the boundary conditions (37d) and (37f) describe the situation in which $(\partial\mathscr{B})_{\rm C}$, besides being undeformable, is also impermeable to the fluid and to the nutrients. Finally, the Dirichlet condition (37g), with $\omega_{\rm Nenv}$ kept constant in all calculations, means that the tissue specimen finds itself in a "bath" of nutrients, which can flow through the boundary surfaces $(\partial\mathscr{B})_{\rm Left}$ and $(\partial\mathscr{B})_{\rm Right}$.

Together with (37a)–(37g), we enforce the initial conditions:

$$\chi^r(R,\Theta,Z,0) = R, \quad \chi^\vartheta(R,\Theta,Z,0) = \Theta, \tag{38a}$$
$$\chi^z(R,\Theta,Z,0) = Z + u_{\rm in}(Z), \tag{38b}$$
$$p(R,\Theta,Z,0) = 0, \tag{38c}$$
$$\omega_{\rm N}(R,\Theta,Z,0) = \omega_{\rm Nenv}, \tag{38d}$$
$$\gamma(R,\Theta,Z,0) = \gamma_{\rm in}(Z), \tag{38e}$$
$$\omega_{\rm p}(R,\Theta,Z,0) = 1, \tag{38f}$$

which apply at all inner points of $\mathscr{B}$. The way in which the problem is formulated allows to infer that the deformation gradient tensor takes on the form $\boldsymbol{F} = \boldsymbol{e}_r \otimes \boldsymbol{E}^R + \boldsymbol{e}_\vartheta \otimes \boldsymbol{E}^\Theta + (1+u')\boldsymbol{e}_z \otimes \boldsymbol{E}^Z$, where u is the axial displacement, the prime indicates partial differentiation in the axial direction (i.e., $u' \equiv \partial u/\partial Z$), while $\{\boldsymbol{e}_r, \boldsymbol{e}_\vartheta, \boldsymbol{e}_z\}$ and $\{\boldsymbol{E}^R, \boldsymbol{E}^\Theta, \boldsymbol{E}^Z\}$ are the vector basis and the co-vector basis generated by the coordinate systems $\hat{x} = (r, \vartheta, z)$ and $\hat{X} = (R, \Theta, Z)$, respectively. It is understood that $R \in [0, R_{\rm in}]$, $\Theta \in [0, 2\pi[$, and $Z \in \left[-\frac{1}{2}L, \frac{1}{2}L\right]$.

As a further simplification, we require that all the physical quantities involved in the model are point-independent on each cross-section of the specimen, whereas they *do* vary along the axis of the cylinder, i.e., they are point-dependent only through the axial coordinate, Z. Therefore, the scalar curvature reads

$$\kappa_\gamma = \frac{2(\gamma')^2 - 4\gamma\gamma''}{\gamma^4} = \frac{6(\gamma')^2 - (4\gamma\gamma')'}{\gamma^4}, \tag{39}$$

and the model equations simplify as reported below:

$$[(\boldsymbol{P}_{\rm sc})^{zZ}]' = p', \tag{40a}$$
$$\dot{\overline{1+u'}} = \left[\frac{k_0}{1+u'}\,p'\right]', \tag{40b}$$
$$[(1+u') - \gamma^3\Phi_{{\rm s}\nu}]\dot{\omega}_{\rm N} = \left[\left(\frac{(1+u') - \gamma^3\Phi_{{\rm s}\nu}}{(1+u')^2} d_{0{\rm R}}\right)\omega_{\rm N}'\right]' + \gamma^3\Phi_{{\rm s}\nu}\left[3\frac{\dot{\gamma}}{\gamma}\omega_{\rm N} - \frac{\zeta_{\rm Np}}{\varrho_{\rm f}}\frac{\omega_{\rm N}}{\omega_{\rm N}+\omega_{\rm N0}}\omega_{\rm p}\right], \tag{40c}$$
$$\dot{\omega}_{\rm p} = -\frac{\zeta_{\rm pn}}{\varrho_{\rm s}}\left\langle 1 - \frac{\omega_{\rm N}}{\omega_{\rm Ncr}}\right\rangle_+ \omega_{\rm p} + \frac{\zeta_{\rm nf}}{\varrho_{\rm s}}[1-\omega_{\rm p}] + 3[1-\omega_{\rm p}]\frac{\dot{\gamma}}{\gamma}, \tag{40d}$$
$$\frac{\dot{\gamma}}{\gamma} = |c|\left[\frac{\zeta_{\rm fp}}{3\varrho_{\rm s}}\frac{\omega_{\rm N}}{\omega_{\rm Ncr}}\frac{(1+u') - \gamma^3\Phi_{{\rm s}\nu}}{(1+u')(1-\Phi_{{\rm s}\nu})}\omega_{\rm p}\right]\frac{4\gamma\gamma'' - 2(\gamma')^2}{\gamma^4}$$

$$+\frac{\zeta_{\mathrm{fp}}}{3\varrho_{\mathrm{s}}}\left\langle\frac{\omega_{\mathrm{N}}-\omega_{\mathrm{Ncr}}}{\omega_{\mathrm{Nenv}}-\omega_{\mathrm{Ncr}}}\right\rangle_{+}\left[1-\frac{\delta_1\langle\bar{\sigma}\rangle_{+}}{\delta_2+\langle\bar{\sigma}\rangle_{+}}\right]\frac{(1+u')-\gamma^3\Phi_{\mathrm{s}\nu}}{(1+u')(1-\Phi_{\mathrm{s}\nu})}\omega_{\mathrm{p}}$$
$$-\frac{\zeta_{\mathrm{nf}}}{3\varrho_{\mathrm{s}}}[1-\omega_{\mathrm{p}}], \tag{40e}$$

where we have set $J = 1 + u'$, and k_0 is defined in (22a). Equations (40a)–(40d) are now put in weak form, and solved by employing the Finite Element Method. To eliminate rigid motions along the axial direction, we introduce a Dirichlet point for u at $Z = 0$, where we prescribe $u(0, t) = 0$ for all t. Finally, we assign the initial conditions $\gamma_{\mathrm{in}}(Z)$ and $u_{\mathrm{in}}(Z)$ in such a way that the problem results to be symmetric with respect to $Z = 0$.

Parameter	Unit	Value	Equation	Reference
L	[cm]	1.000	Initial length	—
R_{in}	[cm]	$1.000 \cdot 10^{-2}$	Initial radius	—
λ	[Pa]	$1.333 \cdot 10^{4}$	(27)	[70]
μ	[Pa]	$1.999 \cdot 10^{4}$	(27)	[70]
k_0	[mm^4/(N s)]	0.4875	(22a), (23a),	[66]
m_0	[−]	0.0848	(22a)	[66]
m_1	[−]	4.638	(22a)	[66]
$d_{0\mathrm{R}}$	[m^2/s]	$3.200 \cdot 10^{-9}$	(22b), (40c)	[66]

Table 1: Parameters used in the definitions of the energy density, permeability and diffusivity. The mass fraction of the solid phase in the natural state is $\Phi_{\mathrm{s}\nu} = 0.8$. The solid and fluid phase densities are $\varrho_{\mathrm{s}} = \varrho_{\mathrm{f}} = 1000$ kg/m^3.

5. Results

To evaluate the impact of the scalar curvature, κ_γ, on the evolution of the system under study, we solve (40a)–(40e) twice: First, we set $c = 0$ in (40e), thereby switching off the term with κ_γ (this first model is denominated M1). Then, we set $c \neq 0$, and solve (40a)–(40e), paying particular attention to the effect of κ_γ (this second model is referred to as M2).

For our purposes, we prepare a protocol of numerical experiments in which the initial distribution of the growth-related distortions, $\gamma_{\mathrm{in}}(Z)$, has strong gradients and non-vanishing curvatures. Specifically, we consider two types of $\gamma_{\mathrm{in}}(Z)$, i.e.,

$$\gamma_{\mathrm{osc}}(Z) = f_0 + g_0\cos(h_0 Z), \tag{41a}$$
$$\gamma_{\mathrm{atan}}(Z) = \begin{cases} a_0 - b_0\,\mathrm{atan}\big(r_0\left(Z+\frac{1}{4}L\right)\big), & Z \in \left[-\frac{1}{2}L, 0\right], \\ a_0 + b_0\,\mathrm{atan}\big(r_0\left(Z-\frac{1}{4}L\right)\big), & Z \in \left]0, \frac{1}{2}L\right], \end{cases} \tag{41b}$$

Parameter	Unit	Value	Description	Reference
ζ_{fp}	$[\mathrm{kg}/(\mathrm{m}^3\,\mathrm{s})]$	$1.343 \cdot 10^{-3}$	(31d),(33),(42)	[71]
ζ_{pn}	$[\mathrm{kg}/(\mathrm{m}^3\,\mathrm{s})]$	$1.500 \cdot 10^{-3}$	(31a)	[71]
ζ_{nf}	$[\mathrm{kg}/(\mathrm{m}^3\,\mathrm{s})]$	$1.150 \cdot 10^{-5}$	(31b)	[71]
ζ_{Np}	$[\mathrm{kg}/(\mathrm{m}^3\,\mathrm{s})]$	$3.000 \cdot 10^{-4}$	(31c)	[72, 73]
c	$[\mathrm{m}^2]$	$\{0, -10^{-6}\}$	(33)	—
g_0	$[-]$	$0.125 \cdot 10^{-1}$	(41a)	—
f_0	$[-]$	$1 + g_0$	(41a)	—
h_0	$[1/\mathrm{cm}]$	$8\,\pi$	(41a)	—
a_0	$[-]$	1.020	(41b)	—
b_0	$[-]$	0.010	(41b)	—
r_0	$[1/\mathrm{cm}]$	$50\,\pi$	(41b)	—
ω_{Ncr}	$[-]$	$1.000 \cdot 10^{-3}$	(31d), (33),(42)	—
ω_{Nenv}	$[-]$	$7.000 \cdot 10^{-3}$	(31d),(42)	—
ω_{N0}	$[-]$	$1.480 \cdot 10^{-4}$	(31c)	—
δ_1	$[-]$	$7.138 \cdot 10^{-1}$	(31d),(42)	[74]
δ_2	[Pa]	$1.541 \cdot 10^{3}$	(31d),(42)	[74]

Table 2: Parameters used in the definitions of the system's geometry, in the definitions of the sources and sinks of mass, and in the initial conditions for γ.

both defining even functions with respect to $Z = 0$, and representing a grown configuration of the tumour characterised by strong inhomogeneities. All the parameters featuring in (41a) and (41b) are reported in Table 2. The models 'M1' and 'M2' are further specialised in 'M1(a)' and 'M2(a)', for $\gamma_{\mathrm{in}} = \gamma_{\mathrm{osc}}$, and 'M1(b)' and 'M2(b)', for $\gamma_{\mathrm{in}} = \gamma_{\mathrm{atan}}$.

5.1. Formulation of specialised sub-models

Models M1(a) and M1(b) [no spatial resolution of the inhomogeneities]. We solve (40a)–(40e) with $c = 0$, thereby switching off the curvature in the simulations. Hence, (40e) reduces to the ordinary differential equation

$$\begin{aligned}\frac{\dot{\gamma}}{\gamma} =& \frac{\zeta_{\mathrm{fp}}}{3\varrho_{\mathrm{s}}} \left\langle \frac{\omega_{\mathrm{N}} - \omega_{\mathrm{Ncr}}}{\omega_{\mathrm{Nenv}} - \omega_{\mathrm{Ncr}}} \right\rangle_+ \left[1 - \frac{\delta_1 \langle \bar{\sigma} \rangle_+}{\delta_2 + \langle \bar{\sigma} \rangle_+}\right] \frac{(1+u') - \gamma^3 \Phi_{\mathrm{s}\nu}}{(1+u')(1-\Phi_{\mathrm{s}\nu})} \omega_{\mathrm{p}} \\ & - \frac{\zeta_{\mathrm{nf}}}{3\varrho_{\mathrm{s}}}[1 - \omega_{\mathrm{p}}], \end{aligned} \tag{42}$$

and the boundary condition (37h) is no longer necessary. Therefore, together with (40a)–(40d) and (42), only the boundary conditions (37a)–(37g) and the initial conditions (38a)–(38f) have to be accounted for.

Although the spatial variability of γ does not play a direct role on (42), the initial distribution of the growth-related distortions *does* influence the evolution of γ.

Models M2(a) and M2(b) [spatial resolution of the inhomogeneities]. We solve (40a)–(40e) with $c \neq 0$, and we enforce the complete set of boundary and initial conditions, i.e., (37a)–(37h) and (38a)-(38f), respectively. In this case, the scalar curvature, κ_γ, *does* contribute to drive the evolution of γ, through the first term on the right-hand-side of (40e).

5.2. Numerical results

In Fig. 2, we report the displacement of the tumour in the axial direction of the specimen, evaluated at the cross section of the cylinder $Z = L/2$, i.e., $u(L/2, t) = \chi^z(L/2, t) - \chi^z(L/2, 0)$. As expected, in all the considered cases, the results of our simulations show that $u(L/2, t)$ increases monotonically with time. By comparing M1(a) with M2(a), and M1(b) with M2(b), we note that the curvature seems to play a significant role in the evolution of the tumour displacement. In fact, the inclusion of the curvature augments the steepness of the displacement from the beginning of the simulation, and, from the 3rd day onward, it increases its magnitude appreciably. This result suggests, in addition, that the initial curvature relaxes, and that the system, at the end of the simulation, finds itself in a less curved configuration.These deductions are confirmed by Fig. 3 and Fig. 4, in which the spatial distribution of the scalar curvature κ_γ, at the initial and final instants of time, is presented.

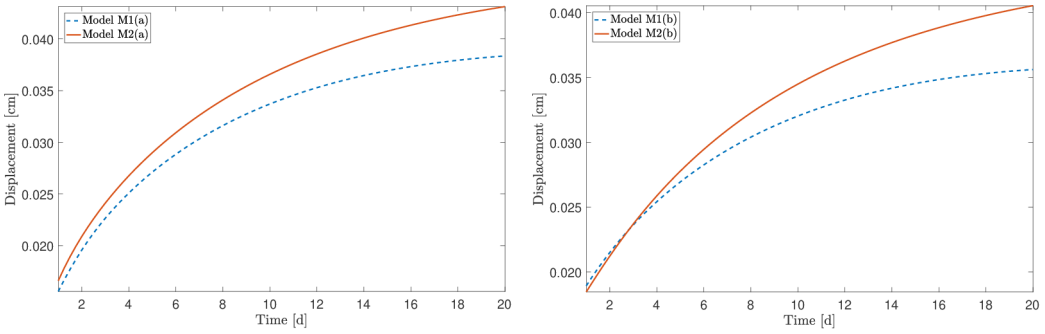

Figure 2: Evolution of the tumour in the axial direction, evaluated at the cross section $Z = L/2$. Panel on the left: comparison between M1(a) and M2(a), for which $\gamma_{\text{in}} = \gamma_{\text{osc}}$. Panel on the right: comparison between M1(b) and M2(b), for which $\gamma_{\text{in}} = \gamma_{\text{atan}}$.

Starting from Fig. 3, we note that the oscillating behaviour of the scalar curvature κ_γ, which reflects the trend of the initial distribution of the inhomogeneities $\gamma_{\text{in}} = \gamma_{\text{osc}}$, results strongly mitigated at the end of the simulation. In fact, oscillations are appeased in this case, and κ_γ is closer to zero than the initial case, which means that tissue is evolving towards a configuration with reduced curvature. Analogously, in Fig. 4, the concentration of the gradient, which characterizes the scalar curvature for the model with $\gamma_{\text{in}} = \gamma_{\text{osc}}$,

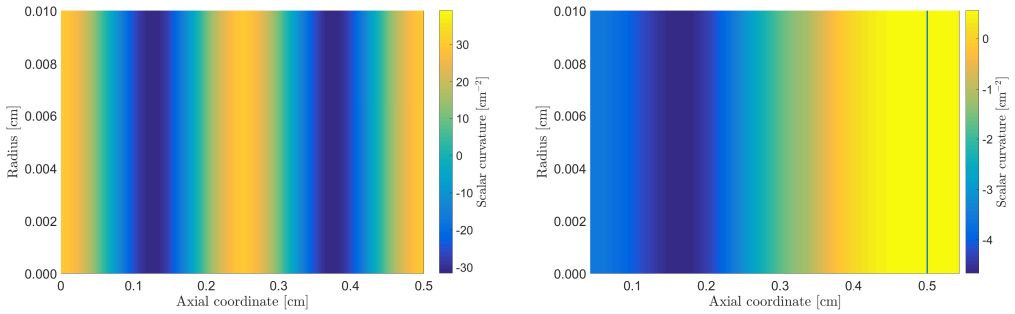

Figure 3: Spatial distribution of the scalar curvature κ_γ evaluated on the meridian section of the specimen, in the case of $\gamma_{\text{in}} = \gamma_{\text{osc}}$. Panel on the left: initial instant of time. Panel on the right: final instant of time.

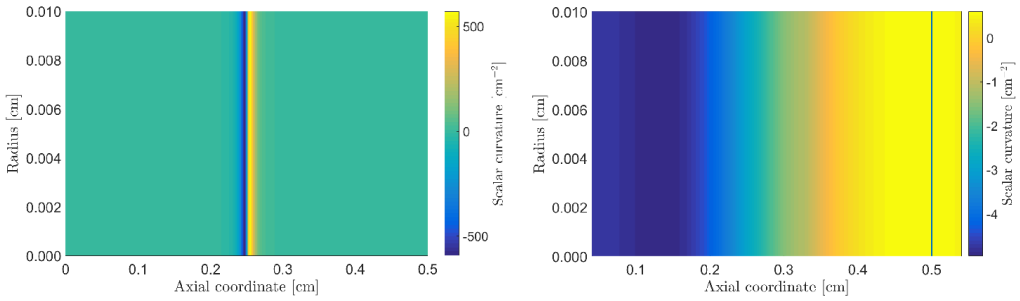

Figure 4: Spatial distribution of the scalar curvature κ_γ evaluated on the meridian section of the specimen, in the case of $\gamma_{\text{in}} = \gamma_{\text{atan}}$. Panel on the left: initial instant of time. Panel on the right: final instant of time.

relaxes at the end of the simulation. Also in this case, the tissue attains a final configuration in which the inhomogeneities are appreciably redistributed. The presence of the curvature κ_γ in the model and its relaxation, influences the spatial trend of the growth. In this sense, looking at Fig. 5, we notice that marked qualitative differences emerge among the spatial profiles of γ computed with M1(a) and M2(a), or M1(b) and M2(b). Still, if we neglect the embodiment of the curvature, the curves are qualitatively similar, with the magnitude increasing as time goes by. In particular, no peculiarity of the initial data seems to be found in the computed curves: The presence of oscillations in the case for which $\gamma_{\text{in}} = \gamma_{\text{osc}}$ (left), or the steep change in concavity, for the other choice of γ_{in}, i.e. $\gamma_{\text{in}} = \gamma_{\text{atan}}$ (right). On the other hand, when the curvature is explicitly considered, the spatial distribution of the growth is strongly influenced by the initial conditions. In detail, depending on time, the oscillations (left) and the rapid change in concavity (right), characterizing the two chosen initial distribution of inhomogeneities, are mitigated, but still present, until the end of the simulations. Althougth

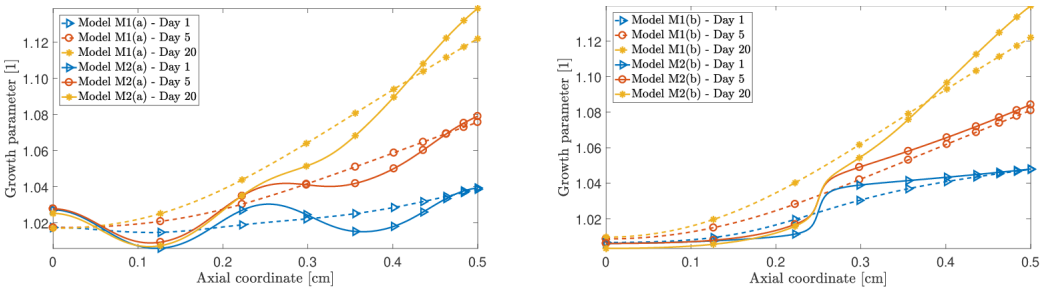

Figure 5: Spatial profile of the growth parameter γ for the models with $\gamma_{\text{in}} = \gamma_{\text{osc}}$ (panel on the left) and $\gamma_{\text{in}} = \gamma_{\text{atan}}$ (panel on the right). Since the problem is symmetric, only the half $[0, L/2]$ of the domain is shown.

the differences outlined above, and independently on the initial condition γ_{in}, all the considered models lead to a final spatial behaviour of γ, in which the inhomogeneities are present.

Another point to put in evidence concerns Fig. 5 (left). The sub-system corresponding to the interval $[0, L/2]$ is initially symmetric with respect to $Z = L/4$. Yet, this further symmetry is lost in the course of time, as visible from the the spatial profile of γ. This peculiarity of the results could be explained by referring to biological motivations, rather than geometric ones. To specify this aspect, let us focus on Fig. 6, which reports the trend of the nutrient mass fraction. We note, indeed, that the nutrients tend to diffuse from the boundaries $(\partial\mathscr{B})_{\text{Left}}$ and $(\partial\mathscr{B})_{\text{Right}}$ towards the centre of the specimen, along its axial direction. In the course of this process, there exists an instant of time after which the mass fraction of the nutrients becomes smaller than the critical value ω_{Ncr} in the interior of the tumour. Hence, while the growth of the tumour is inhibited in its centre, it is active close to the free boundaries, where the mass fraction of the nutrients is still higher than the critical threshold.

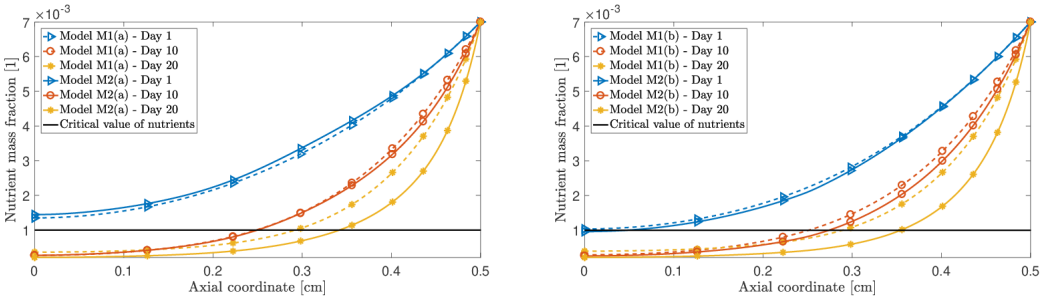

Figure 6: Spatial profile of the nutrient mass fraction ω_{N} for the models with $\gamma_{\text{in}} = \gamma_{\text{osc}}$ (panel on the left) and $\gamma_{\text{in}} = \gamma_{\text{atan}}$ (panel on the right). Since the problem is symmetric, only the half $[0, L/2]$ of the domain is shown.

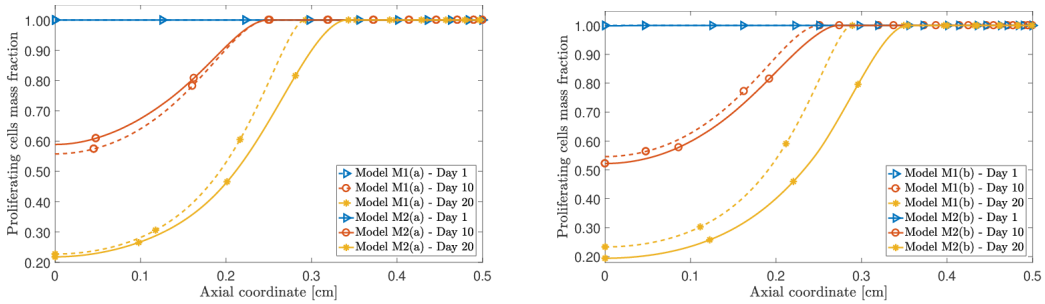

Figure 7: Spatial profile of the proliferating cells mass fraction ω_{P} for the models with $\gamma_{\mathrm{in}} = \gamma_{\mathrm{osc}}$ (panel on the left) and $\gamma_{\mathrm{in}} = \gamma_{\mathrm{atan}}$ (panel on the right). Since the problem is symmetric, only the half $[0, L/2]$ of the domain is shown.

A relevant result concerns the dynamics of the proliferating cells, as shown in Fig. 7. Their mass fraction, ω_{p}, remains close to unity in the proximity of the boundary $(\partial\mathscr{B})_{\mathrm{Right}}$, where the level of nutrients is still high, while it diminishes in the centre of the tumour, where nutrients tend to become unavailable (this means that the proliferating cells are "converted" into necrotic ones). This phenomenon is influenced by the explicit resolution of the curvature in the model. Indeed, when the curvature is explicitly considered, the conversion process of proliferating cells into necrotic ones is accelerated in the first days, and slowed down towards the end of the simulations. This behaviour occurs for both choices of γ_{in}, but appears to be slightly more pronounced for $\gamma_{\mathrm{in}} = \gamma_{\mathrm{atan}}$.

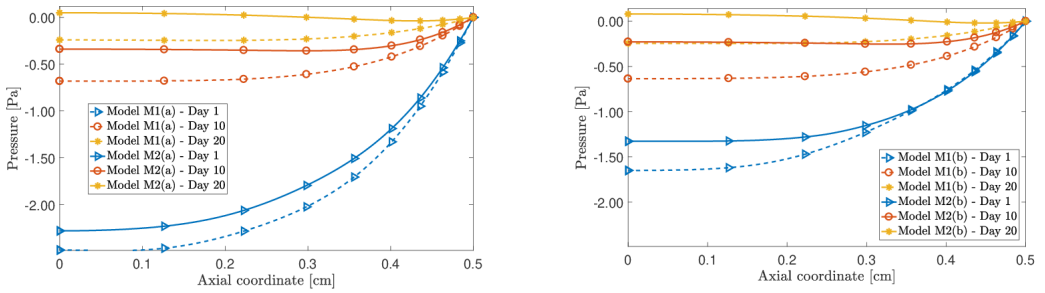

Figure 8: Spatial profile of the pore pressure p for the models with $\gamma_{\mathrm{in}} = \gamma_{\mathrm{osc}}$ (panel on the left) and $\gamma_{\mathrm{in}} = \gamma_{\mathrm{atan}}$ (panel on the right). Since the problem is symmetric, only the half $[0, L/2]$ of the domain is shown.

To proceed with our analysis, we refer to Fig. 8, where we plot the behaviour of the pressure, p. When the tumour grows, the interstitial fluid flows towards the centre of the tumour, and p decreases from the free boundary (where the condition $p = 0$ applies) to the tumour's interior, where it takes on negative values. However, when the system goes towards the end of the

simulations, p tends to become positive in the cases in which the curvature is explicitly accounted for, while it tends to zero from below otherwise.

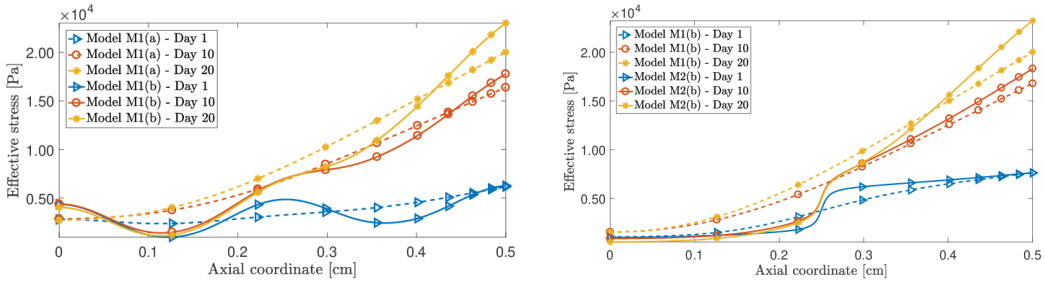

Figure 9: Spatial profile of the effective stress $\bar{\sigma}$ for the models with $\gamma_{\text{in}} = \gamma_{\text{osc}}$ (panel on the left) and $\gamma_{\text{in}} = \gamma_{\text{atan}}$ (panel on the right). Since the problem is symmetric, only the half $[0, L/2]$ of the domain is shown.

Finally, in Fig. 9, we display the effective stress $\bar{\sigma}$. First, we notice that the tumour is subjected to a compressive stress, since $\bar{\sigma}$ is positive. Apart from this result, which is common to all the studied cases, we report that the curvature modifies the qualitative behaviour of $\bar{\sigma}$. As final remark, we note how the spatial evolution of the stress in the specimen, independently of the model, is strongly affected by the initial distribution of the inhomogeneities.

6. Conclusion

In this work, a mathematical model addressing tumour growth has been presented. The mechanical framework has been developed by regarding the tumour as a multi-constituent, biphasic medium, and by enforcing the BKL-decomposition of the deformation gradient tensor. The growth of the tumour is influenced by both mechanical stimuli and biological factors, such as the nutrients transported by the interstitial fluid, and the interactions among proliferating and necrotic cells.

The principal novelty of our approach consists of a partial reformulation of the balance laws for the constituents of the solid phase, in such a way that it is introduced an explicitly dependence on the scalar curvature, κ_γ, generated by the growth tensor $\boldsymbol{U}_\gamma = \gamma \boldsymbol{I}$ through the Riemannian, growth-related metric tensor $\boldsymbol{C}_\gamma = \gamma^2 \boldsymbol{G}$.

The introduction of κ_γ amounts to express the evolution law for γ as a partial differential equation, with the purpose of obtaining a better resolution of the material inhomogeneities, and an estimate of their influence on growth. To accomplish this task, we prescribe two types of initial conditions for γ, both characterised by strong gradient and nonzero initial curvature, $\kappa_{\gamma\text{in}}$.

Two more thoughts about our results may be worth to be mentioned. The first one concerns the physical interpretation of the evolution of the initial inhomogeneities accompanying γ_{in}. Indeed, since γ evolves according to a generalised diffusion-reaction like equation, one may say that, in our model, the material inhomogeneities brought about by growth "dissipate" towards a configuration in which they are redistributed over the tissue. The second thought pertains to the structure of the evolution equation (40e), and is also related to the first one. Indeed, in the case in which the initial inhomogeneities relax, the system tends to pass from a configuration in which it is not invariant under material translations to a homogeneous configuration in which it is translational invariant, thereby restoring the symmetry that is initially broken by γ_{in}.

One limitation of our study is related to the fact that, in this work, we have just relied on a phenomenological model in which κ_γ appears without a strong theoretical justification. We have not built a systematic constitutive framework, in which, for example, the strain energy density of our material depends on γ *and* on κ_γ, nor have we conducted any study of the dissipation inequality of the system at hand. Yet, confident in the intuitions that have led to the model presented in [42], we hope that our results could provide a basis for further investigations.

In our work, we concentrated on an academic benchmark problem in order to compare our results with those of other Authors and, in particular, with those of Ambrosi and Mollica [55]. For this reason, our general setting is *as* simple *as* the setting of the problems taken as reference, expect for the fact that we deal with a biphasic system featuring two cell populations and for the fact that we account for the role of inhomogeneities through the introduction of the term $r_{\text{p}\gamma}$ in the mass balance law of the proliferant cells. Clearly, our model can be further generalised and, in our opinion, this could be done in several steps. Here, we give some indications on how the formulation of our problem should look like if such generalisations were done.

First, one could consider exactly the same framework and geometry as the ones presented here, while relaxing the hypothesis of axial symmetry of the problem. In this case, the initial inhomogeneities may vary not only in the axial direction, but also radially or circumferentially, and the scalar curvature κ_γ must be computed according to its own definition (6), since it is no longer represented by (39). This requires the computation of all the partial derivatives necessary to determine the Christoffel symbols as well as the fourth-order curvature tensor specified in (4) and (5), respectively.

A second option could be to formulate an evolution law for γ in which the evolution is driven by the full curvature tensor $\boldsymbol{\mathcal{R}}$ and its gradient $\text{Grad}\boldsymbol{\mathcal{R}}$, rather than by the scalar curvature only. In this case, the definitions of $r_{\text{p}\gamma}$

and $r_{\mathrm{n}\gamma}$ should be further generalised, thereby implying a rewriting of the mass balance laws of the proliferant and necrotic cells.

A further extension of the model could be the formulation of an evolution law for the whole growth tensor $\boldsymbol{F}_\gamma$, with a restriction on $\mathrm{tr}[\dot{\boldsymbol{F}}_\gamma \boldsymbol{F}_\gamma^{-1}]$, as done in (10b). A model of this type extends the concept of growth presented in this work and further rephrases the theory proposed in [42].

Another step is to specialise our model to problems with more realistic geometries, which may arise from two- and three-dimensional studies. For a given study, this means that the boundary value problem formulated in our work has to be modified, and the Finite Element scheme adopted to solve it has to be extended accordingly. In particular, the use of new computational schemes may not be needed to resolve physical phenomena that could not be captured otherwise, as is the case, for example, when the growth of a tumour in the present of a host tissue and is studied [54].

Finally, although in the present work we dispensed with remodelling from the outset, we are aware of the fact that such process accompanies growth. In fact, it plays an important role in the redistribution of the mechanical stress within the tissue and, thus, on the modulating effect of the latter on the growth of a tumour. One possible way for studying remodelling is to use the decompositions $\boldsymbol{F} = \boldsymbol{F}_{\mathrm{e}}\boldsymbol{F}_{\mathrm{r}}\boldsymbol{F}_\gamma$ or as $\boldsymbol{F} = \boldsymbol{F}_{\mathrm{e}}\boldsymbol{F}_\gamma\boldsymbol{F}_{\mathrm{r}}$, where $\boldsymbol{F}_{\mathrm{r}}$ represents the distortion tensor describing the remodelling process, and to study the dynamics of $\boldsymbol{F}_{\mathrm{r}}$ in relationship with all the other model variables. In the literature, $\boldsymbol{F}_{\mathrm{r}}$ is often assumed to describe a plastic-like phenomenon and is thus treated accordingly. Within the context of tumour growth, $\boldsymbol{F}_{\mathrm{r}}$ accounts for the structural transformations of a tissue at the cellular level. Its introduction requires to elaborate numerical schemes capable of capturing the interplay between the growth and the structural evolution of a tissue, even when these phenomena exhibit rather separated time scales.

Moreover, our model could be developed and extended to describe other biological situations. For instance, the approach presented in this work for isotropic media could be adapted for describing a tumour growing in anisotropic tissues. Moreover, we could investigate the coupling with other remodelling phenomena, introduced in term of cellular reorganisation, bluefibre reorientation or onset of degenerative phenomena. Finally, at the pore scale, the effect of inhomogeneities could be studied by introducing a kinematic descriptor, called "*intrinsic volume ratio*" [64].

Conflict of Interests

The Authors declare that they have no conflict of interests.

Acknowledgments

We thank Prof. Marcelo Epstein (The University of Calgary, Canada) for proficuous discussions, which helped us in the understanding of his work.

Article information

DOI: 10.1016/j.ijnonlinmec.2018.08.003. Available online: August 10, 2018. Journal: *International Journal of Non-Linear Mechanics* 106 (2018) 174-187

References

[1] R. P. Araujo, D. L. McElwain, A history of the study of solid tumour growth: the contribution of mathematical modelling, Bulletin of Mathematical Biology`doi:10.1016/s0092-8240(03)00126-5`.

[2] T. Alarcón, H. Byrne, P. Maini, A cellular automaton model for tumour growth in inhomogeneous environment, Journal of Theoretical Biology 225 (2) (2003) 257–274. `doi:10.1016/s0022-5193(03)00244-3`.

[3] G. W. Jones, S. J. Chapman, Modeling growth in biological materials, SIAM Review 54 (1) (2012) 52–118. `doi:10.1137/080731785`.

[4] A. Guerra, D. Rodriguez, S. Montero, J. Betancourt-Mar, R. Martin, E. Silva, M. Bizzarri, G. Cocho, R. Mansilla, J. Nieto-Villar, Phase transitions in tumor growth VI: Epithelial–mesenchymal transition, Physica A: Statistical Mechanics and its Applications 499 (2018) 208–215. `doi:10.1016/j.physa.2018.01.040`.

[5] N. Bellomo, L. Preziosi, Modelling and mathematical problems related to tumor evolution and its interaction with the immune system, Mathematical and Computer Modelling 32 (3-4) (2000) 413–452. `doi:10.1016/s0895-7177(00)00143-6`.

[6] H. M. Byrne, M. A. Chaplain, Growth of nonnecrotic tumors in the presence and absence of inhibitors., Mathematical biosciences 130 (1995) 151–181.

[7] H. Byrne, D. Drasdo, Individual-based and continuum models of growing cell populations: a comparison, Journal of Mathematical Biology 58 (4-5) (2009) 657–687. `doi:10.1007/s00285-008-0212-0`.

[8] P. Macklin, S. McDougall, A. R. A. Anderson, M. A. J. Chaplain, V. Cristini, J. Lowengrub, Multiscale modelling and nonlinear simulation of vascular tumour growth, Journal of Mathematical Biology 58 (4-5) (2009) 765–798. doi:10.1007/s00285-008-0216-9.

[9] T. Roose, S. J. Chapman, P. K. Maini, Mathematical models of avascular tumor growth, SIAM Review 49 (2) (2007) 179–208. doi:10.1137/s0036144504446291.

[10] D. Ambrosi, G. Ateshian, E. Arruda, et al., Perspectives on biological growth and remodeling, J. Mech. Phys. Solids 59(4) (2011) 863–883. doi:10.1016/j.jmps.2010.12.011.

[11] J. D. Humphrey, Towards a theory of vascular growth and remodeling, in: H. G.A., O. R.W. (Eds.), Mechanics of Biological Tissue, Springer-Verlag, 2006, pp. 3–15. doi:10.1007/3-540-31184-x_1.

[12] H. Byrne, L. Preziosi, Modelling solid tumour growth using the theory of mixtures, Mathematical Medicine and Biology 20 (4) (2003) 341–366. doi:10.1093/imammb/20.4.341.

[13] L. Preziosi, G. Vitale, A multiphase model of tumor and tissue growth including cell adhesion and plastic reorganization, Math. Models Methods Appl. Sci. 21 (09) (2011) 1901–1932. doi:10.1142/s0218202511005593.

[14] D. Ambrosi, L. Preziosi, G. Vitale, The insight of mixtures theory for growth and remodeling, Z. Angew. Math. Phys. 61 (2010) 177–191. doi:10.1007/s00033-009-0037-8.

[15] A. Grillo, S. Federico, G. Wittum, Growth, mass transfer, and remodeling in fiber-reinforced, multi-constituent materials, Int. J. Nonlinear Mech. 47 (2012) 388–401. doi:10.1016/j.ijnonlinmec.2011.09.026.

[16] G. Ateshian, J. Humphrey, Continuum mixture models of biological growth and remodeling: Past successes and future opportunities, Annual Review of Biomedical Engineering 14 (1) (2012) 97–111. doi:10.1146/annurev-bioeng-071910-124726.

[17] R. D. O'Dea, S. L. Waters, H. M. Byrne, A multiphase model for tissue construct growth in a perfusion bioreactor, Mathematical Medicine and Biology 27 (2) (2010) 95–127. doi:10.1093/imammb/dqp003.

[18] D. Ambrosi, S. Pezzuto, D. Riccobelli, T. Stylianopoulos, P. Ciarletta, Solid tumors are poroelastic solids with a chemo-mechanical feedback on growth, J. Elast. 129 (2017) 107–124. doi:10.1007/s10659-016-9619-9.

[19] A. DiCarlo, S. Quiligotti, Growth and balance, Mechanics Research Communications 29 (6) (2002) 449–456. doi:10.1016/s0093-6413(02)00297-5.

[20] S. C. Cowin, G. A. Holzapfel, On the modeling of growth and adaptation, in: H. G. A., O. R. W. (Eds.), Mechanics of Biological Tissue, Springer-Verlag, 2006, pp. 29–46. doi:10.1007/3-540-31184-x_3.

[21] A. Guillou, R. W. Ogden, Growth in soft biological tissue and residual stress development, in: G. Holzapfel, R. Ogden (Eds.), Mechanics of Biological Tissue, Springer-Verlag, 2006, pp. 47–62. doi:10.1007/3-540-31184-x_4.

[22] G. A. Ateshian, On the theory of reactive mixtures for modeling biological growth, Biomechanics and Modeling in Mechanobiology 6 (6) (2007) 423–445. doi:10.1007/s10237-006-0070-x.

[23] P. Ciarletta, M. Destrade, A. L. Gower, On residual stresses and homeostasis: an elastic theory of functional adaptation in living matter, Scientific Reports 6 (1). doi:10.1038/srep24390.

[24] E. Kuhl, Growing matter: A review of growth in living systems, J. Mech. Behav. Biomed. Mater. 29 (2014) 529–543. doi:10.1016/j.jmbbm.2013.10.009.

[25] J. D. Humphrey, K. R. Rajagopal, A constrained mixture model for growth and remodeling of soft tissues, Mathematical Models and Methods in Applied Sciences 12 (03) (2002) 407–430. doi:10.1142/s0218202502001714.

[26] E. Rodriguez, A. Hoger, A. McCulloch, Stress-dependent finite growth in soft elastic tissues, J. Biomech. 27 (1994) 455–467. doi:https://doi.org/10.1016/0021-9290(94)90021-3.

[27] L. A. Taber, Biomechanics of growth, remodeling, and morphogenesis, Applied Mechanics Reviews 48 (8) (1995) 487. doi:10.1115/1.3005109.

[28] M. Epstein, G. A. Maugin, Thermomechanics of volumetric growth in uniform bodies, International Journal of Plasticity 16 (7-8) (2000) 951–978. doi:10.1016/s0749-6419(99)00081-9.

[29] K. Garikipati, E. Arruda, K. Grosh, H. Narayanan, S. Calve, A continuum treatment of growth in biological tissue: the coupling of mass transport and mechanics, J. Mech. Phys. Solids 52 (2004) 1595–1625. doi:10.1016/j.jmps.2004.01.004.

[30] B. Loret, F.M.F. Simões, A framework for deformation, generalized diffusion, mass transfer and growth in multi-species multi-phase biological tissues, Eur. J. Mech. A 24 (2005) 757–781. doi:10.1016/j.euromechsol.2005.05.005.

[31] R. K. Jain, J. D. Martin, T. Stylianopoulos, The role of mechanical forces in tumor growth and therapy, Annu. Rev. Biomed. Eng. 16 (2014) 321–346. doi:10.1146/annurev-bioeng-071813-105259.

[32] M. Böl, A. B. Albero, On a new model for inhomogeneous volume growth of elastic bodies, J. Mech. Beh. Biom. Mat. 29 (2014) 582–593. doi:10.1016/j.jmbbm.2013.01.027.

[33] A. Ramírez-Torres, R. Rodríguez-Ramos, J. Merodio, J. Bravo-Castillero, R. Guinovart-Díaz, J. Alfonso, Mathematical modeling of anisotropic avascular tumor growth, Mechanics Research Communications 69 (2015) 8–14. doi:10.1016/j.mechrescom.2015.06.002.

[34] A. Grillo, R. Prohl, G. Wittum, A poroplastic model of structural reorganisation in porous media of biomechanical interest, Continuum Mech. Therm. 28 (2016) 579–601. doi:10.1007/s00161-015-0465-y.

[35] A. Grillo, R. Prohl, G. Wittum, A generalised algorithm for anelastic processes in elastoplasticity and biomechanics, Math. Mech. Solids 22(3) (2017) 502–527. doi:10.1177/1081286515598661.

[36] M. Mićunović, Thermomechanics of Viscoplasticity, Springer New York, 2009. doi:10.1007/978-0-387-89490-4.

[37] S. Sadik, A. Yavari, On the origins of the idea of the multiplicative decomposition of the deformation gradient, Mathematics and Mechanics of Solids 22 (4) (2017) 771–772. doi:10.1177/1081286515612280.

[38] E. Kröner, Allgemeine Kontinuumstheorie der Versetzungen und Eigenspannungen, Archive for Rational Mechanics and Analysis 4 (1) (1959) 273–334. doi:10.1007/bf00281393.

[39] A. Klarbring, T. Olsson, J. Stålhand, Theory of residual stresses with application to an arterial geometry, Arch. Mech. 59(4–5) (2007) 341–364.

[40] A. Yavari, A geometric theory of growth mechanics, J. Nonlinear Sci. 20 (2010) 781–830. doi:10.1007/s00332-010-9073-y.

[41] A. Yavari, A. Goriely, Weyl geometry and the nonlinear mechanics of distributed point defects, Proc. R. Soc. A 468 (2012) 3902–3922. doi:10.1098/rspa.2012.0342.

[42] M. Epstein, Self-driven continuous dislocations and growth, in: M. G. Steinmann P. (Ed.), Mechanics of Material Forces. Advances in Mechanics and Mathematics, Vol. 11, Springer, Boston, MA, 2005, pp. 129–139. doi:10.1007/0-387-26261-x_13.

[43] P. Ciarletta, D. Ambrosi, G. Maugin, Mass transport in morphogenetic processes: A second gradient theory for volumetric growth and material remodeling, J. Mech. Phys. Solids 60 (2012) 432–450. doi:10.1016/j.jmps.2011.11.011.

[44] M. Minozzi, P. Nardinocchi, L. Teresi, V. Varano, Growth-induced compatible strains, Math. Mech. Solids 22 (1) (2016) 62–71. doi:10.1177/1081286515570510.

[45] A. Goriely, The Mathematics and Mechanics of Biological Growth, Springer New York, 2016. doi:10.1007/978-0-387-87710-5.

[46] P. Nardinocchi, L. Teresi, V. Varano, The elastic metric: A review of elasticity with large distortions, Int. J. Nonlinear Mech. 56 (2013) 34–42. doi:10.1016/j.ijnonlinmec.2013.05.002.

[47] J. Lubliner, Plasticity Theory, Dover Publications, Inc., Mineola, New York, 2008.

[48] M. Epstein, M. Elźanowski, Material Inhomogeneities and their Evolution — A Geometric Approach, 1st Edition, Springer-Verlag Berlin Heidelberg, 2007. doi:10.1007/978-3-540-72373-8.

[49] M. Epstein, The geometric language of continuum mechanics, Cambridge University Press, 2010.

[50] A. Menzel, Modelling of anisotropic growth in biological tissues — a new approach and computational aspects, Biomechan. Model. Mechanobiol. 3 (2005) 147–171. doi:10.1007/s10237-004-0047-6.

[51] T. Olsson, A. Klarbring, Residual stresses in soft tissue as a consequence of growth and remodeling: application to an arterial geometry, Eur. J. Mech. A 27(6) (2008) 959–974. doi:10.1016/j.euromechsol.2007.12.006.

[52] C. Voutouri, F. Mpekris, P. Papageorgis, A. D. Odysseos, T. Stylianopoulos, Role of constitutive behavior and tumor-host mechanical interactions in the state of stress and growth of solid tumors, PLoS ONE 9 (8) (2014) e104717. doi:10.1371/journal.pone.0104717.

[53] F. Mpekris, S. Angeli, A. P. Pirentis, T. Stylianopoulos, Stress-mediated progression of solid tumors: effect of mechanical stress on tissue oxygenation, cancer cell proliferation, and drug delivery, Biomech. Model. Mechanobiol. 14 (6) (2015) 1391–1402. doi:10.1007/s10237-015-0682-0.

[54] P. Mascheroni, M. Carfagna, A. Grillo, D. Boso, B. Schrefler, An avascular tumor growth model based on porous media mechanics and evolving natural states, Mathematics and Mechanics of Solids 23 (4) (2018) 686–712. doi:10.1177/1081286517711217.

[55] D. Ambrosi, L. Preziosi, On the closure of mass balance models for tumor growth, Mathematical Models and Methods in Applied Sciences 12 (05) (2002) 737–754. doi:10.1142/s0218202502001878.

[56] D. Ambrosi, F. Mollica, The role of stress in the growth of a multicell spheroid, J. Math. Biol. 49 (2004) 477–499. doi:10.1007/s00285-003-0238-2.

[57] C. Giverso, M. Scianna, A. Grillo, Growing avascular tumours as elasto-plastic bodies by the theory of evolving natural configurations, Mech. Res. Commun. 68 (2015) 31–39. doi:http://dx.doi.org/10.1016/j.mechrescom.2015.04.004.

[58] G. Helmlinger, P. A. Netti, H. C. Lichtenbeld, R. J. Melder, R. K. Jain, Solid stress inhibits the growth of multicellular tumor spheroids, Nature Biotechnology 15 (8) (1997) 778–783. doi:10.1038/nbt0897-778.

[59] S. Preston, M. Elzanowski, Material uniformity and the concept of the stress space, in: B. Albers (Ed.), Continuous Media with Microstructure, 1st Edition, Springer-Verlag Berlin Heidelberg, 2010, pp. 91–101. doi:10.1007/978-3-642-11445-8.

[60] V. Ciancio, M. Dolfin, M. Francaviglia, S. Preston, Uniform materials and the multiplicative decomposition of the deformation gradient in finite elasto-plasticity, J. Non-Equilib. Thermodyn. 33(3) (2008) 199–234. doi:10.1515/JNETDY.2008.009.

[61] J. Marsden, T. Hughes, Mathematical Foundations of Elasticity, Dover Publications, Inc., Mineola, New York, 1983.

[62] L. S. Bennethum, M. A. Murad, J. H. Cushman, Macroscale thermodynamics and the chemical potential for swelling porous media, Transport in Porous Media 39 (2) (2000) 187–225. doi:10.1023/a:1006661330427.

[63] G. Sciarra, G. A. Maugin, K. Hutter, A variational approach to a microstructured theory of solid-fluid mixtures, Archive of Applied Mechanics 73 (2003) 194–224. doi:10.1007/s00419-003-0279-4.

[64] R. Serpieri, F. Travascio, Variational continuum multiphase poroelasticity, Springer Singapore, 2017. doi:10.1007/978-981-10-3452-7.

[65] G. Ateshian, J. Weiss, Anisotropic hydraulic permeability under finite deformation, J. Biomech. Engng. 132 (2010) 111004–1–111004–7. doi:10.1115/1.4002588.

[66] M. H. Holmes, V. C. Mow, The nonlinear characteristics of soft gels and hydrated connective tissues in ultrafiltration., Journal of biomechanics 23 (1990) 1145–1156. doi:10.1016/0021-9290(90)90007-P.

[67] S. Cleja-Tigoiu, G. A. Maugin, Eshelby's stress tensors in finite elastoplasticity, Acta Mechanica 139 (1-4) (2000) 231–249. doi:10.1007/bf01170191.

[68] A. Tomic, A. Grillo, S. Federico, Poroelastic materials reinforced by statistically oriented fibres — numerical implementation and application to articular cartilage, IMA J. Appl. Math. 79 (2014) 1027–1059. doi:10.1093/imamat/hxu039.

[69] A. Bazykin, Nonlinear dynamics of interacting populations, World Scientific Publishing, Singapore New Jersey London Hong Kong, 1998.

[70] T. Stylianopoulos, J. D. Martin, M. Snuderl, F. Mpekris, S. R. Jain, R. K. Jain, Coevolution of solid stress and interstitial fluid pressure in tumors during progression: Implications for vascular collapse, Cancer Research 73 (13) (2013) 3833–3841. doi:10.1158/0008-5472.can-12-4521.

[71] M. A. J. Chaplain, L. Graziano, L. Preziosi, Mathematical modelling of the loss of tissue compression responsiveness and its role in solid tumour development, Mathematical Medicine and Biology: A Journal of the IMA 23 (3) (2006) 197–229. doi:10.1093/imammb/dql009.

[72] J. J. Casciari, S. V. Sotirchos, R. M. Sutherland, Mathematical modelling of microenvironment and growth in EMT6/ro multicellular tumour spheroids, Cell Proliferation 25 (1) (1992) 1–22. doi:10.1111/j.1365-2184.1992.tb01433.x.

[73] J. J. Casciari, S. V. Sotirchos, R. M. Sutherland, Variations in tumor cell growth rates and metabolism with oxygen concentration, glucose concentration, and extracellular pH, Journal of Cellular Physiology 151 (2) (1992) 386–394. doi:10.1002/jcp.1041510220.

[74] P. Mascheroni, C. Stigliano, M. Carfagna, D. P. Boso, L. Preziosi, P. Decuzzi, B. A. Schrefler, Predicting the growth of glioblastoma multiforme spheroids using a multiphase porous media model, Biomech. Model. Mechanobiol. 15 (5) (2016) 1215–1228. doi:10.1007/s10237-015-0755-0.